Effective connectivity in the neural pathways for reading: A case study

Nicholas Henry Neufeld, BSc (Hons)

Advisors: Prof Cathy Price and Dr Mohamed Seghier

Wellcome Trust Centre for Neuroimaging
Institute of Neurology
University College London

Submitted as partial fulfillment of the requirements for the
MSc in Clinical Neuroscience, University of London
2008

MSc Clinical Neuroscience
2007/08

ProQuest LLC
789 East Eisenhower Parkway
P.O. Box 1346
Ann Arbor, MI 48106-1346

Acknowledgments

It is altogether appropriate to begin by thanking the Commonwealth Scholarship Commission in the United Kingdom and the Canadian Bureau for International Education at Foreign Affairs Canada. I would not have been able to pursue this course nor undertake this research had it not been for receiving the Commonwealth Scholarship.

Further gratitude is due to the Education Unit at the Institute of Neurology. In particular, I would like to thank Daniela Warr Schori for her help with administrative hurdles throughout the academic year (and before the year even started). I'd also like to extend my gratitude to Dr. Caroline Selai and Dr. Stephanie Schorge for their guidance throughout my time in London.

At the Wellcome Trust Centre for Neuroimaging, I owe Dr. Mohamed Seghier my sincere gratitude for his patience while teaching me Dynamic Casual Modelling and his help in handling data. Last but certainly not least, a huge thank-you to Professor Cathy Price for taking me onboard and allowing me to wrestle with a new neuroimaging method. Through Professor Price's mentorship I had the pleasure of witnessing the technical skills that make a great neuroimager and the character that makes a great scientist.

Statement of Contributions

Study Design: Cathy Price

Data Collection: Cathy Price

Data Analysis: Nicholas Neufeld, Mohamed Seghier

Write-Up: Nicholas Neufeld

Table of Contents

Abbreviations

ATP	adenosine triphosphate
BF	Bayes factor
BOLD	blood oxygenation level dependent
DCM	Dynamic Causal Model
DTI	Diffusion Tensor Imaging
EEG	electroencephalogram
EPI	echo planar imaging
FWHM	full width half maximum
fMRI	functional Magnetic Resonance Imaging
FOV	field of view
GLM	general linear model
GRE	gradient echo
iOCC	inferior occipital region
MNI	Montreal Neurological Institute
MR	magnetic resonance
MRI	Magnetic Resonance Imaging
p1	ventral post-central region
p2	ventral pre-central region
PER	positive evidence ratio
SNR	signal-to-noise ratio
sOCC	superior occipital region
SPM	Statistical Parametric Mapping
STS	superior temporal sulcus region
TE	echo time
TMS	transcranial magnetic stimulation
TR	time to repeat
VOI	volume of interest
VWFA	visual word form area

1 Abstract

The current study investigates the case of AH, a patient who in 2001 sustained a venous thrombosis leading to secondary haemorrhage and consequent left occipito-temporal brain damage. Previous studies implicated the damaged region in reading, yet despite the patient's lesion, some reading ability was preserved. According to the model of reading put forth by Cohen *et al.* (2003), successful reading is normally dependent upon a left occipito-temporal region called the visual word form area (VWFA). This area allows strings of visual stimuli (letters) to be read in parallel. When the left VWFA is damaged, a putative right VWFA was proposed to preserve reading by functioning with left hemisphere language areas and allowed letters to be read serially. The preserved reading ability in AH did not fit the Cohen model on the basis of neuropsychological investigations. Drawing on previous functional magnetic resonance imaging (fMRI) results, AH did not activate the putative right VWFA, yet overactivation was observed in other right and left hemisphere regions relative to neurologically normal controls. The current study employed the new technique of Dynamic Causal Modelling (DCM) to model the effective connectivity between regions in which AH showed greater activation during reading when compared with controls. Contrary to the model of Cohen and colleagues, a ventral pathway in the left hemisphere was discovered that did not go through either VWFA. This result provided an alternative model of preserved reading abilities within the left hemisphere. Rehabilitation techniques may benefit from such results insofar as reading strategies can be assigned to preserved pathways in patients.

2 Introduction

> To the Reader.
> This Figure, that thou here seest put,
> It was for gentle Shakespeare cut;
> Wherein the Grauer had a strife
> with Nature, to out-doo the life:
> O, could he but haue drawne his wit
> As well in brasse, as he hath hit
> His face; the Print would then surpasse
> All, that was euer writ in brasse.
> But, since he cannot, Reader, looke
> Not on his Picture, but his Booke.
> (Shakespeare, 1623)

These few lines can be found in William Shakespeare's First Folio, a work published seven years after Shakespeare's death. The poem is on the preface's left page while an engraving of Shakespeare's bust is on the right. To paraphrase, the writer explains to the reader that he is unable to capture Shakespeare's essence in his engraving. To understand Shakespeare it would be better to read Shakespeare's book. For modern literary scholars, this poem and other preliminaries of the time are largely responsible for the practice of using literary texts as a means of interpreting an author's life. While the written word can aid in understanding the author, the read word can aid in understanding the reader.

2.1 Reading and the Brain

There are 150 million items housed at the British Library and nearly 400,000 people flock to the Library each year to see everything from Shakespeare's First Folio to modern literature (British Library, 2008). Yet as remarkable as the items are, all the more remarkable is the ability of people to read them. Normal reading and vision are tightly coupled. From a historical view, reading emerged less than 5000 years ago while universal literacy appeared roughly a hundred years ago (Dronkers *et al.*, 2000). From an

evolutionary view, the recency of reading suggests it is subserved by connections between the visual and language systems rather than a system solely devoted to reading (Dronkers *et al.*, 2000).

The development of links between vision and language underlie the acquisition of reading (Cohen *et al.*, 2003). Visually, the brain must learn how to quickly identify letters and words. Such visual identification must occur for different fonts or forms and under different viewing conditions. Verbally, the brain must learn how to divide the speech stream into discrete units like syllables and phonemes (Morais and Kolinsky, 1994). Strings of letters and sounds become associated, as do strings of letters and lexical entries in memory. Together, this allows new words to be sounded out and associated with knowledge of familiar words (Cohen *et al.*, 2003).

There are two types of reading strategies in adults: parallel and serial. Parallel reading involves the rapid identification of a group of letters. Evidence for parallel reading comes from word length studies. Within a range of approximately three to six letters, the amount of time required to read any word is roughly constant (Weekes, 1997; Lavidor and Ellis, 2002). From a developmental view, it takes roughly five years of instruction to establish this parallel reading strategy (Aghababian and Nazir, 2000). Indeed, a word length effect, such that longer words take longer to read, is said to remain at least until a child is ten years old (Aghababian and Nazir, 2000).

When words are greater than the capacity for a parallel strategy, reading times are linearly related to word length (Cohen *et al.*, 2003). This suggests that reading proceeds by a serial (letter-by-letter) strategy in which the reader must perceive each letter separately before forming the target word. Serial reading may occur for words greater

than six letters, however it is abnormal for adults to serially read words between three and six letters long (Cohen *et al.*, 2003). Nevertheless, brain lesions may result in serial reading when parallel reading would normally be employed.

The disruption of reading following a brain lesion is known as alexia and may occur in combination with a disruption in writing (agraphia) or on its own (Dronkers *et al.*, 2000). Furthermore, alexia may be combined with or separate from impaired understanding or production of speech (aphasia). Commonly, alexic patients are able to write spontaneously or to dictation within the range of controls (Cohen *et al.*, 2003). In addition, alexics commonly retain their abilities to comprehend and produce oral language (Cohen *et al.*, 2003). While alexics commonly show normal ranges for writing and oral language, deviations from normal reading are observed. At the extreme end, patients with global alexia cannot identify single letters (Dejerine, 1891, 1892). Less severely affected patients retain letter identification yet read using the aforementioned serial strategy. In these patients, the lesion site and serial reading strategy indicate that a region involved in parallel reading has been damaged while a region involved in serial reading is preserved. The work of Laurent Cohen and colleagues (2003) has given the framework for interpreting such results.

2.2 The Cohen Model

According to Cohen *et al.* (2003), letters presented to one hemifield are analyzed through a cascade of contralateral retinotopic cortical regions. These regions process increasingly abstract representations of the letters until an invariant representation of a word is created. The cortical location for words is in what Cohen and colleagues have dubbed the visual word form area (VWFA). The VWFA is thought to be located within

the left occipito-temporal sulcus and employed during the parallel reading strategy. Phonological or lexico-semantic processing of words then occurs through projections from the VWFA to other cortical regions. Of relevance to rehabilitation, the homologous region in the right hemisphere (R-VWFA) is thought to take over the function of the left VWFA and allow for serial reading. Functional recovery from alexia is then proposed to result from an alternative right hemisphere pathway (Figure 2.2) (Cohen *et al.*, 2003).

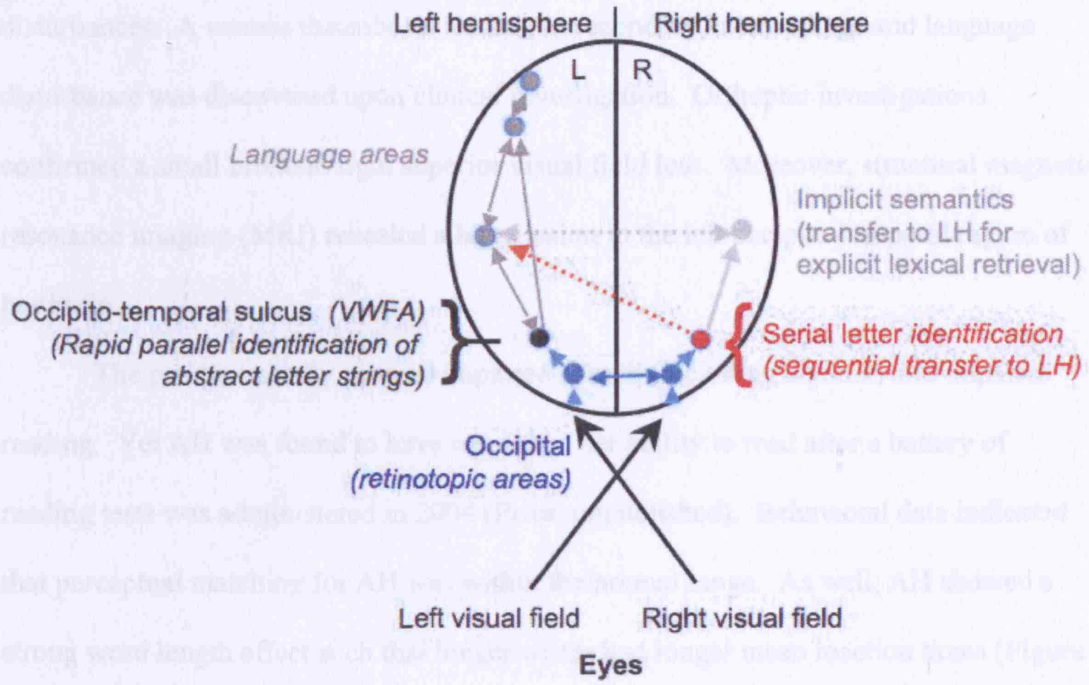

Figure 2.2: The model of Cohen *et al.* (2003) suggests that words are initially processed in contralateral retinotopic occipital regions (blue dots). The rapid parallel reading strategy can then be executed in the left Visual Word Form Area (VWFA), shown above as a black dot. Phonological and lexico-semantic properties can then be added to words by projections to other cortical regions (grey dots). Damage to the left occipito-temporal region forces reading to be accomplished by serial letter identification, a process hypothesized by Cohen and colleagues to be executed by the right VWFA (red dot).

2.3 Patient AH

The current study documents the functional recovery of an alexic. In January 2001, AH, a 49-year-old woman, presented to hospital staff with a headache and visual disturbances. A venous thrombosis leading to secondary haemorrhage and language disturbance was discovered upon clinical investigation. Orthoptic investigations confirmed a small bilateral right superior visual field loss. Moreover, structural magnetic resonance imaging (MRI) revealed a large lesion in the left occipito-temporal region of her brain.

The patient initially showed impaired speech (including anomia) and impaired reading. Yet AH was found to have recovered her ability to read after a battery of reading tests was administered in 2004 (Price, unpublished). Behavioral data indicated that perceptual matching for AH was within the normal range. As well, AH showed a strong word length effect such that longer words had longer mean reaction times (Figure 2.3.1). The neuropsychological inferences thus suggested the functional deficit occurred after normal perception and resulted in serial reading. However, the slow pace AH exhibited was consistent yet too fast for a serial reading strategy (Price, unpublished). Hence it appeared that AH retained some parallel reading. As well, when forcing AH to read faster, AH was more accurate at reading aloud than making semantic decisions.

Contrary to this neuropsychological inference, AH's lesion was in the same region that neurologically normal controls activate during a perceptual matching task in a functional magnetic resonance imaging (fMRI) experiment (Price, unpublished). Furthermore, the lesion covered the occipito-temporal region, a region that neurologically normal controls activate during reading short high frequency words (Figure 2.3.2). Thus,

fMRI suggested AH was able to read despite damage to regions implicated in normal perceptual and language processing.

REACTION TIMES TO VARIABLE WORD LENGTHS IN PATIENT AH

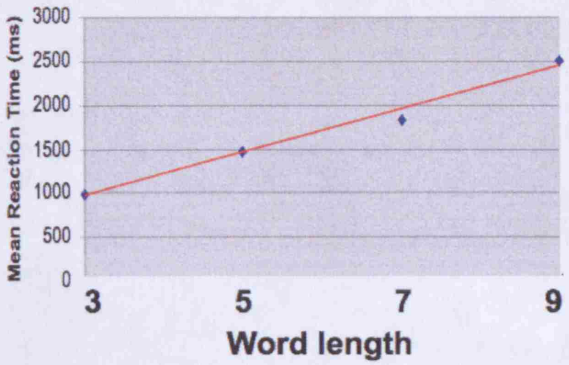

Figure 2.3.1: Reading times were linearly related to word length in patient AH. This was consistent with a serial reading strategy. Nonetheless, the speed at which AH was able to read remained higher than what would be expected for a serial reading strategy (Price, unpublished).

NORMAL ACTIVATION FOR SHORT HIGH FREQUENCY WORDS

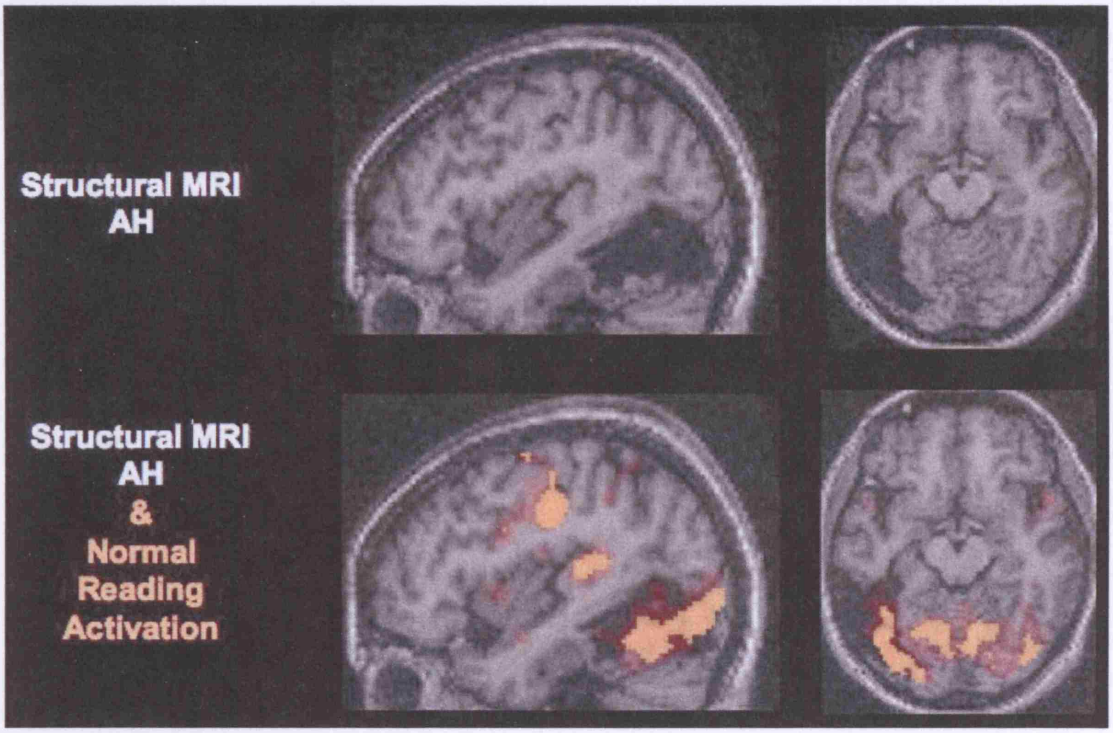

Figure 2.3.2: A venous thrombosis with secondary haemorrhage can result in uncommon lesion sites. In patient AH, a venous thrombosis with secondary haemorrhage resulted in a large lesion covering much of the occipito-temporal region. AH is able to read despite damage to areas normally activated for reading single, short, high frequency words.

According to Cohen *et al.* (2003), a lesion to the left occipito-temporal cortex disrupts rapid parallel letter identification (Figure 2.3.3a). A patient with such a lesion would presumably show a word length effect due to reliance on the intact right hemisphere supporting serial processing. A lesion to the left and right occipito-temporal regions would result in global alexia (Figure 2.3.3b). Similarly, a lesion to the left occipito-temporal region and posterior corpus callosum would result in global alexia (Figure 2.3.3c).

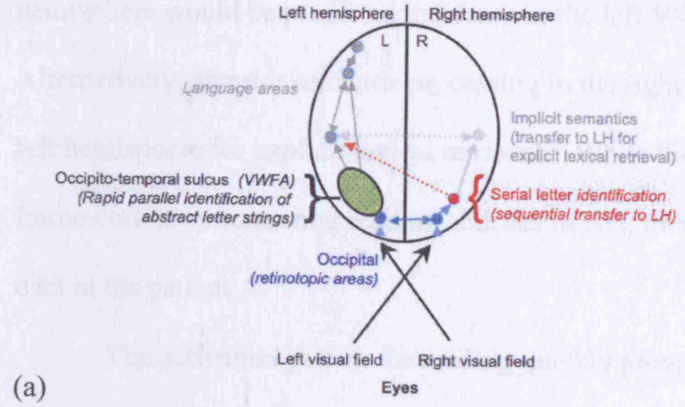

(a)

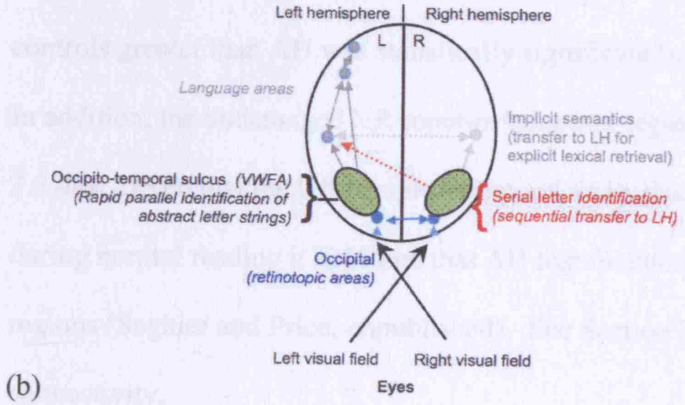

(b)

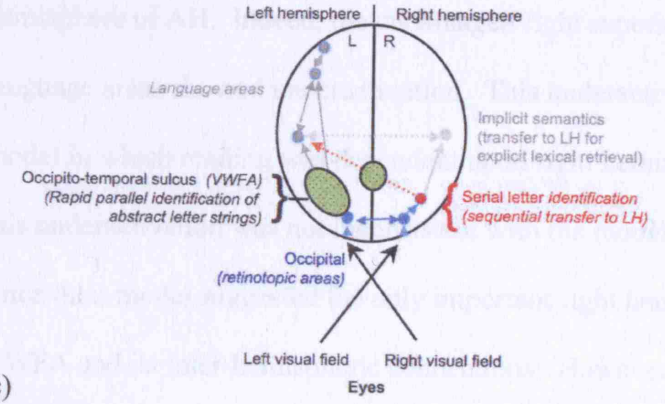

(c)

Figure 2.3.3: The model proposed by Cohen *et al.* (2003) yields three major predictions for patients with lesions (green) in regions implicated in reading: (a) the patient shows a serial reading strategy due to a damaged left Visual Word Form Area (VWFA) and reliance on the right VWFA, (b) the patient suffers from global alexia and is unable to read due to damage of the left and right VWFAs, or (c) the patient suffers from global alexia and is unable to read due to damage of the left VWFA and corpus callosum.

The damage AH sustained to the occipito-temporal region would have eliminated the left VWFA. However, according Cohen and colleagues, the intact VWFA in the right hemisphere would be predicted to take over the left VWFA and allow for reading. Alternatively, anterior semantic processing in the right hemisphere would project to the left hemisphere for explicit lexical retrieval. While these predictions provide a framework for interpreting reading abilities in AH, they are not corroborated by fMRI data in the patient.

The activation pattern for reading quickly provides an overview of potential reading pathways in patient AH (Figure 2.3.4). Not surprisingly, AH's damaged left occipito-temporal region was seen to underactivate relative to controls (i.e. the contrast of controls greater than AH was statistically significant in the left occipito-temporal region). In addition, the undamaged left superior temporal region showed underactivation (Figure 2.3.4a). Given that the left occipito-temporal and superior temporal activation correlated during normal reading it appeared that AH lost functional connectivity between these two regions (Seghier and Price, unpublished). See Section 3.2 for a discussion on functional connectivity.

Referring to Figure 2.3.4b, underactivation was also present in the right hemisphere of AH. Indeed, the undamaged right superior temporal and premotor language areas showed underactivation. This underactivation was inconsistent with a model in which reading was dependent upon right hemisphere language areas. However, this underactivation was not inconsistent with the model proposed by Cohen *et al.* (2003) since their model suggested the only important right hemisphere regions were the right VWFA and its inter-hemispheric connections. However, no right VWFA activation was

found when AH was compared with controls. Despite this, AH showed overactivation compared to controls in a more posterior and inferior occipital region in the right hemisphere (i.e. the contrast of AH greater than controls was statistically significant in the right posterior inferior occipital cortex).

(a)

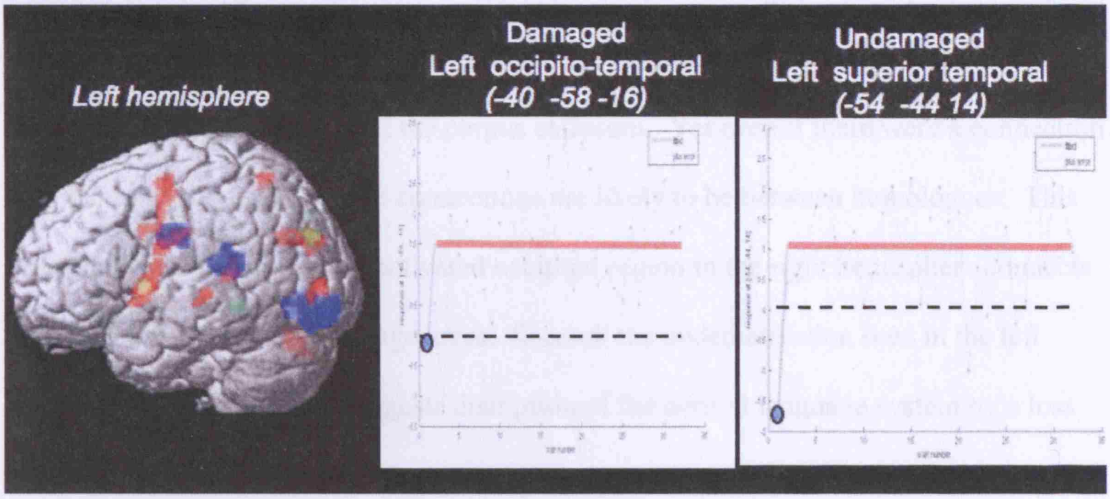

(b)

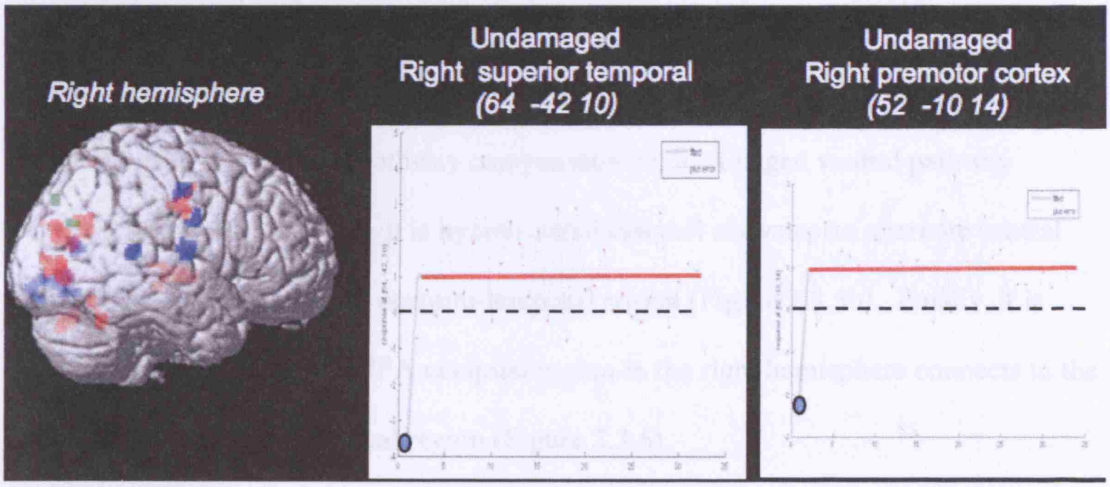

Figure 2.3.4: AH was seen to underactivate in several regions implicated in reading. Activation patterns are overlaid on the template brain provided in SPM. Red activation corresponds to regions activated by AH and controls ($p < 0.001$). Green and yellow activation corresponds to regions activated in AH more than controls ($p < 0.05$, uncorrected). Blue activation corresponds to regions only activated by controls ($p < 0.05$ corrected). Underactivated regions are shown in the four graphs. Note the blue dot refers to patient AH while the red line refers to the mean activation for controls and the black dashes refer to the zero line.

There are then two major problems in applying Cohen and colleagues' model to AH. First, AH's right occipital activation is posterior to the right VWFA proposed by Cohen *et al.* (2003). There is also no anatomical evidence that the right VWFA has connections via the splenium of the corpus callosum. Yet even if there were a connection with the corpus callosum, these connections are likely to be between homologues. This raises the question of how the activated occipital region in the right hemisphere connects with the left hemisphere language areas. Second, the underactivation seen in the left hemisphere language areas suggests disruption of the normal language system by a loss of inputs to the left VWFA. This raises the question of which left hemisphere regions are involved in reading.

Taking these problems into consideration, the current study aims to test three competing hypotheses that model the effective connectivity for reading in patient AH. It is hypothesized that a dorsal pathway compensates for a damaged ventral pathway (Figure 2.3.5a). Alternatively, it is hypothesized that AH activates an alternate ventral pathway that bypasses the left occipito-temporal region (Figure 2.3.5b). Finally, it is hypothesized that the non-VWFA occipital region in the right hemisphere connects to the left hemisphere via a subcortical region (Figure 2.3.6).

HYPOTHESIZED LEFT HEMISPHERE PATHWAYS ALLOWING FOR SUCCESSFUL READING IN PATIENT AH

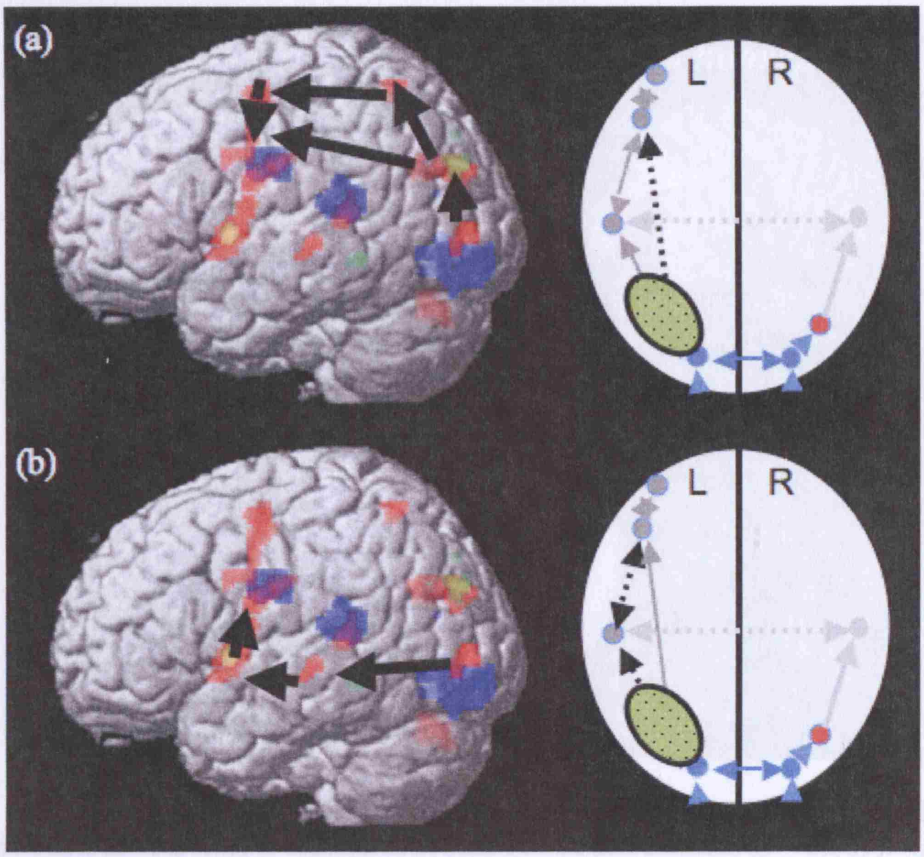

Figure 2.3.5: Activation patterns are overlaid on the template brain provided in SPM. Red activation corresponds to regions activated by AH and controls ($p < 0.001$). Green and yellow activation corresponds to regions more activated in AH than controls ($p < 0.05$, uncorrected). Blue activation corresponds to regions only activated by controls ($p < 0.05$, corrected). Two pathways were hypothesized in AH on the basis of regions that AH and controls activated. (a) One pathway was hypothesized to project from the left occipital cortex, follow a dorsal pathway, and connect with regions in the pre- and post-central gyri. (b) Another pathway was hypothesized to project from the left occipital cortex, follow a ventral pathway, and connect with the aforementioned regions. The precise regions included in the models were determined from areas in which AH overactivated during reading when compared with controls.

HYPOTHESIZED PATHWAYS CONNECTING THE LEFT AND RIGHT HEMISPHERES AND ALLOWING FOR SUCCESSFUL READING IN PATIENT AH

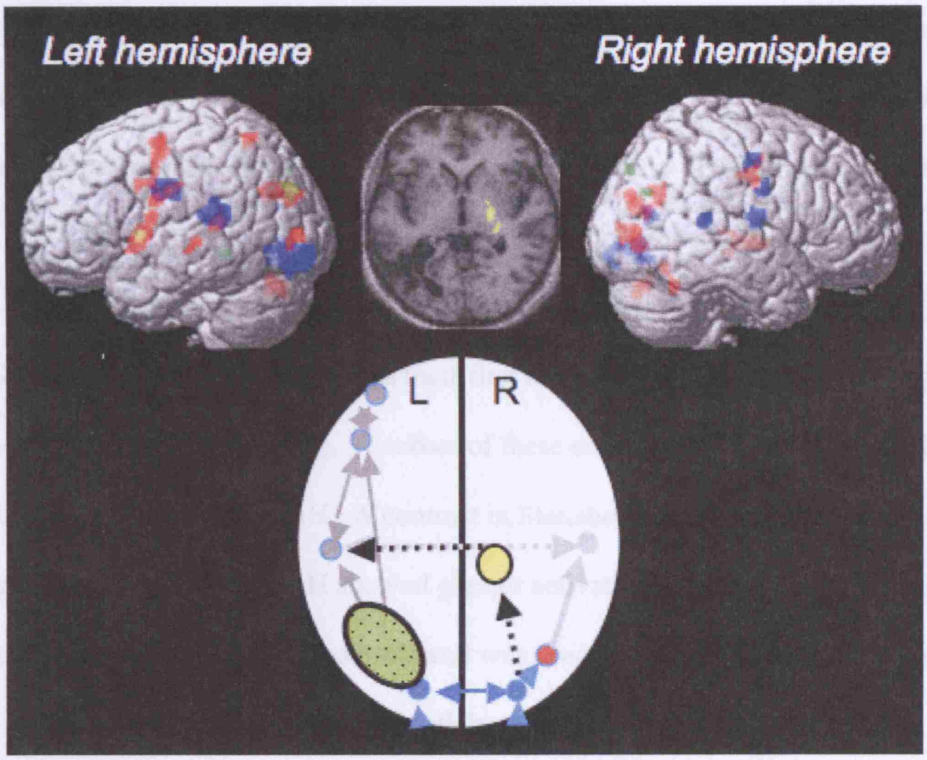

Figure 2.3.6: Activation patterns are overlaid on the template brain provided in SPM. Red activation corresponds to regions activated by AH and controls ($p < 0.001$). Green and yellow activation corresponds to regions more activated in AH than controls ($p < 0.05$, uncorrected). Blue activation corresponds to regions only activated by controls ($p < 0.05$, corrected). Cohen and colleagues' hypothesized right VWFA (red in schematic) was not activated by AH. However, a more inferior and posterior right occipital region (blue in schematic) was overactivated and hypothesized to connect with left hemisphere language areas. The right occipital region was hypothesized to connect with the left hemisphere via the overactivated thalamus (yellow in schematic).

3 Materials and Methods

3.1 Subjects

Patient AH was a right-handed female who suffered a venous thrombosis and secondary haemorrhage leading to alexia when she was 49 years of age. AH was 54 at the time of scanning. See Section 2.3 in the Introduction for a detailed account of the patient.

A total of forty-seven neurologically normal right-handed control subjects (18 males, 29 females) indicated English as their first language and exhibited a wide age-range (M = 30.8 years, SD = 19.0). A subset of these controls was selected on the basis of fMRI activation patterns in AH. A contrast in Statistical Parametric Mapping 5 (SPM 5) compared regions in which AH showed greater activation (overactivation) during reading to neurologically normal controls and was used to define Volumes of Interest (VOIs) for AH. For controls, a custom Matlab script was then used to search up to 6 mm from the coordinates based on the overactivation contrast. Controls were only selected if they showed activation in the same regions as AH. A total of 27 out of 47 controls showed activation in the aforementioned regions. All 27 controls (11 males, 16 females) also exhibited a wide age-range (M = 29.3 years, SD = 16.1).

3.2 Functional Magnetic Resonance Imaging

Functional magnetic resonance imaging measures brain activity indirectly by detecting changes in the signal produced by protons within local tissue. Neuronal firing in response to a given experimental task uses ATP that is replaced through the metabolism of glucose. This metabolism consumes oxygen, thereby reducing oxygen concentration in the surrounding tissue. The brain then detects oxygen consumption and

signals for more oxygen to be delivered by the blood. However, overcompensation occurs when blood flow is increased to active regions of the brain. While metabolism decreases the amount of oxygen in the tissue, the resultant overcompensation of blood flow causes the overall local oxygen concentration to increase. Therefore, in contrast to the basal state, an area of activation will have a higher oxyhaemoglobin to deoxyhaemoglobin ratio. Deoxyhaemoglobin induces dephasing and hence decreases MR signal while, in contrast, active areas have less deoxyhaemoglobin, less dephasing, and more MR signal. Thus, the oxyhaemoglobin to deoxyhaemoglobin ratio serves as an endogenous contrast known as the Blood Oxygenation Level Dependent (BOLD) contrast (Ogawa *et al.*, 1990).

While MR signal changes are observable in response to brain regions performing specific tasks, these signal changes are small compared to the total amount of MR signal. Typically, changes of the MR signal in response to an experimental task account for a few percent of the total signal. Experimental tasks, such as watching a flashing light or squeezing a hand, are considered to elicit robust MR signal changes, yet these signal changes are between 3-5% depending on the field strength of the MR scanner (Ogawa *et al.*, 1993). Thus, given the small changes in MR signal in response to neural activity, experimental designs that increase signal detection are key. While fMRI measures the change in MR signal between control and task periods, a simple subtraction of the control period from the task period is not sufficient to produce statistically significant results for a single event. Several control and task periods must be observed and compared in order to produce a representative MR signal change and increase the statistical significance (Turner *et al.*, 1998).

Block designs serve as one method for detecting MR signal changes. In a block design, participants perform a task repeatedly during one period. This is alternated with control periods. Brain regions are then observed in which the MR signal changes at the expected times. However, it will be noted that the MR signal changes of interest lie on top of large signal. To counteract this, increasing the number of blocks presented to a participant can increase confidence that a brain region is responding to a given experimental task. Importantly, block-related statistical analyses for block designs work well if participants perform all tasks within a block in the same way. Yet there may be differences in the response times between healthy and psychologically interesting participants or clinical populations (Smyser *et al.*, 2001). For example, in a reading task, performance and activation may vary such that in one instance a subject correctly reads a word while in another instance incorrectly reads the word. Block-related analyses are not useful in such cases since activation cannot be separated into correct and incorrect reading trials.

Event-related designs are an alternative to block designs and allow for random stimulus delivery (Buckner *et al.*, 1996, 1998; Rosen *et al.*, 1998). Yet, as in the current study, event-related analyses can be applied to block designs in order for stimuli to be separated in time such that a subject's responses can be isolated. For example, the instances in which a subject reads correctly, and does so quickly, may be separated from the words read incorrectly or words that required more time for reading. Data must be acquired for a longer duration than a typical block design in order for event-related analyses to yield statistically significant results. Expected signal in the fMRI time series may then modeled in the General Linear Model (GLM). This can then be used to

generate a Statistical Parametric Map (SPM) in which an effect of interest is mapped onto a template brain (Friston, 2007a). Regions that are statistically significant give a depiction of functional connectivity. However, these connections are correlative. In contrast, a new methodology has emerged that allows for causal connections to be tested.

3.3 Dynamic Causal Modelling

The concept of functional specialization has been central to fMRI and other neuroimaging modalities (Friston, 2002). With this concept, certain aspects of information processing may be said to be localized in different brain regions. Task-dependent activation patterns are then interpreted as a distributed system. However, as Stephan *et al.* (2007) highlight, functional integration between regions must be considered alongside functional specialization.

One way of characterizing functional integration is through effective connectivity. In general terms, effective connectivity describes the causal influences that one group of neurons exert over another group of neurons (Friston, 1994). Aertsen and Preißl (1991) conceived of effective connectivity as the simplest task and time-dependent circuit diagram that would replicate observed timing relationships between neurons. Common to both of these definitions is the notion of causation. According to Dynamic Causal Modelling (DCM), the task performed by a subject causes neural activity in an input region, thereby eliciting the BOLD response. The neural activity in the input region then causes or modulates neural activity elsewhere in the brain, yielding the overall pattern of BOLD signals. Note the difference here between DCM and standard statistical inference in fMRI using the GLM. In standard fMRI, the pattern of BOLD signals can be interpreted as a *collection* of regions activated during a given task. In DCM, the pattern

of BOLD signals can be interpreted as a *network* of regions that are involved in a given task (Friston *et al.*, 2003, Friston, 2007b).

The aim of DCM is to estimate and make inferences about intrinsic connections between brain regions and how these intrinsic connections are modulated by a task. To do this, DCM begins with a model of how different regions in the brain interact. Stimuli are converted into neuronal dynamics at input regions and a so-called forward model is added. This forward model predicts how neuronal activity results in the observed BOLD signals. The parameters of the model can then be measured, yielding values describing effective connectivity (Friston *et al.*, 2003; Friston, 2007b).

In more technical terms, DCM assumes the brain is a nonlinear dynamic system. This system has inputs, state variables, and outputs. A given experiment is then considered to be a perturbation of this system. While standard fMRI studies (functional connectivity) can have inputs entering anywhere within the model, the effective connectivity modeled in DCM can only have inputs in user-defined regions (Friston *et al.*, 2003; Friston, 2007b).

The state variables in DCM include variables to account for neuronal and other biophysical phenomena that form the outputs. Outputs refer to the observed BOLD signals in user-defined brain regions. The bilinear state equation (Equation 1) models the dynamics of interacting neuronal populations. Integrating the state equation gives predicted neural dynamics that enter a model of the hemodynamic response to give predicted BOLD responses. The parameters at both the neuronal and hemodynamic levels are then adjusted until the differences between predicted and measured BOLD time-series are minimized. Importantly, the neural dynamics are determined by

experimental manipulations. These enter the model in the form of driving inputs. Driving inputs directly elicit local responses that are propagated through the system according to the intrinsic connections. Finally, the strength of these connections can be changed by modulatory inputs such as reading or attention. Since the intrinsic or modulatory connections are rate constants, the strength of a given connection is measured in units of Hertz (Friston *et al.*, 2003; Friston, 2007b).

THE BILINEAR STATE EQUATION OF DCM FOR FMRI

[1] $$\frac{dx}{dt} = (\mathrm{A} + \sum_{j=1}^{m} u_j \mathrm{B}^{(j)})x + \mathrm{C}u$$

Equation 1. Adapted from Stephen *et al.* (2007). Neuronal activity is encoded in the variable x. Thus $\frac{dx}{dt}$ equals the rate of change in neuronal activity. Matrix A encodes the intrinsic connection values that are present in the absence of input. The variable u encodes the external inputs while matrix B encodes the modulatory connection parameters induced by the external inputs. The matrix C encodes the strength inputs directly exert on neuronal activity. Integrating the state equation gives predicted neuronal dynamics that enter a model of the hemodynamic response to give predicted BOLD responses.

Significance values are computed for parameters in matrices A, B, and C. At the single-subject level these values are given in terms of a probability such that a value of 0.95 corresponds to a 95% level of confidence that the parameter is different from zero. Since the current study compared one patient to controls, and since the data from one patient was not robust enough for modulatory connections to reach statistical significance (Appendix 1), only intrinsic connections and their significance were discussed in this study. These intrinsic connections propagated all four tasks through the user-defined regions (see Section 3.4). Hence no conclusions could be made about the extent to which the reading task changed these connections.

After specifying DCMs, the models may be compared using Bayes factors (BF). The Bayes factor is a summary of the amount of evidence in favor of a given model relative to another (Kass and Raftery, 1995). Table 3.3 shows BF values and indicates what can be said of the evidence in favor of a given model. At the group level of analysis, the Positive Evidence Ratio (PER) can be used to gauge the evidence for a given DCM. The PER relates the respective number of subjects with BF values equal to or greater than 3 for two competing DCMs (Table 3.3).

INTEPRETATION OF BAYES FACTORS

BF_{ij}	**Evidence in favor of model *i* over model *j***
1-3	Weak
3-20	Positive
20-150	Strong
≥150	Very Strong

Table 3.3: Adapted from Penny *et al.* (2004). Bayes factors (BF) are relative to the two models being compared. Thus a BF of 1 indicates no decision can be reached about whether hypothesis *i* or *j* is true. A BF of 1-3 corresponds to a 50-75% belief in the statement 'hypothesis *i* is true'. Further, a BF of 3-20 corresponds to a 75-95% belief in the said statement whereas a BF of 20-150 relates a 95-99% belief. Finally, a BF greater than 150 corresponds to a belief greater than 99% that hypothesis *i* is true.

3.4 Experimental Design

Seghier *et al.* (2007, 2008) successfully demonstrated the validity and employed the experimental design used in the current study. Subjects were required to perform four different tasks. First, subjects read aloud three to six letter object names written in English. Second, subjects were shown pictures of objects and asked to name the object aloud. Third, for a visuo-motor baseline, subjects were presented with meaningless pictures of non-objects or symbols in response to which subjects were instructed to say "1, 2, 3". Fourth, subjects fixated on a cross-hair target.

Each subject had two scanning sessions with each session containing four blocks of reading, four blocks of object naming, four blocks of the visuo-motor baseline, and six blocks of fixation baseline. In order to maximize the presentation rate and paradigm efficiency, blocks lasted 18 seconds with 12 stimuli per block presented 3 at a time (i.e. in triads) for 4.5 seconds per triad. Importantly, the items presented during the reading and object naming triads were ensured to have no obvious semantic relationship between the three different items (i.e. slide, axe, cup). The order of conditions was randomized.

3.5 Procedure

The same procedure was performed in the current study as per Seghier *et al.* (2007, 2008) up to second level analyses. A video projector, front-projection screen, and system of mirrors fastened to the head coil were used to present stimuli. Words were presented in lower case Arial font, size 48 with a maximum visual angle on the retina equal to 4.9° x 1.2°. Pictures were scaled to measure between 5-8 cm in width and height with a maximum visual angle on the retina equal to 7.3° x 8.5°. Vocal responses were

recorded during all conditions with a MRI-compatible microphone and sound cancellation system. However, response times were not recorded.

Experiments were performed on a 1.5T Siemens system (Siemens Medical Systems, Erlangen, Germany). Functional scanning was always preceded by 14.4 seconds of dummy scans to insure tissue steady-state magnetization. Functional imaging consisted of an EPI GRE sequence (TR/TE/Flip = 3600 ms/ 50 ms/ 90°, FOV = 192 mm, matrix = 64x64, 40 axial slices, 2 mm thick with 1 mm gap). The EPI GRE sequence used here was optimized to minimize signal dropout by adjusting the slice tilt, the direction of the phase encoding, and the z-shim moment (Weiskopf *et al.*, 2006). To avoid ghost-EPI artifacts, image reconstruction was based on a generalized algorithm (i.e. trajectory-based reconstruction after calibrating a trajectory scan during a gel-phantom experiment).

Data processing and first level analyses were carried out using the SPM 5 software package (Wellcome Trust Centre for Neuroimaging, London UK, http://www.fil.ion.ucl.ac.uk/spm). Functional volumes were spatially realigned, unwarped, normalized to the MNI space, and smoothed with an isotropic 6 mm FWHM Gaussian kernel for both patient AH and controls. Normalized images were resampled to a voxel size of 2x2x2 mm. High-pass filtering (1/128 Hz cutoff) was then used to remove low-frequency noise and signal drift from the time series in each voxel. Statistics were based on a fixed-effect analysis using the GLM in each voxel across the whole brain. Each stimulus onset was modeled as an event and convolved with a canonical hemodynamic response function with no dispersion or temporal derivatives. For each subject, parameter estimates were assessed with least square regression analysis, and the

contrast images were computed for the main effect of reading relative to fixation. Marking a departure from Seghier *et al.* (2007, 2008), eigenvectors (i.e. time series) for volumes of interest (VOIs) were extracted for AH and controls using these first-level analyses.

VOLUMES OF INTEREST INCLUDED IN DCM ANALYSES

VOI	Coordinates (mm)			z-value
Left iOCC	-30	-86	2	3.7
Left sOCC	-24	-80	30	4.5
STS	-64	-30	-4	4.1
p1	-42	-16	28	4.7
p2	-56	4	4	5.7
Right iOCC	28	-76	4	4.5
Right sOCC	26	-70	28	5.2
Right Thalamus	22	-12	-2	4.8

Table 3.5: Coordinates for Volumes of Interest (VOIs) having eigenvectors extracted for patient AH. VOIs were chosen on the basis of significant overactivation during reading in AH relative to controls (z-values). All VOIs were defined as spheres with radii of 4 mm and had a minimum of four activated voxels. For a qualitative comparison, controls had all of the above VOIs extracted, save for the right thalamus. A variable distance of up to 6 mm from patient AH's coordinates allowed the local maxima for each control to be approached and a spherical VOI (radius = 4 mm) defined around the local maxima. Note: iOCC = inferior occipital region, sOCC = superior occipital region, STS = superior temporal sulcus, p1 = ventral post-central region, and p2 = ventral pre-central region.

Second level analysis was performed on patient AH and controls. This revealed areas in which AH overactivated when compared with controls on correct reading trials. Based on the activation pattern, spherical VOIs (radius = 4 mm) in the left hemisphere (five VOIs) and right hemisphere (three VOIs) were extracted in AH (Table 3.5) at local maxima and contained at least four active voxels. Both sessions of the first level contrasts for reading relative to fixation were used when extracting VOIs. This was done at a threshold of $p < 0.05$. Note that the largest DCM here was composed of six VOIs while the maximum number of VOIs included in DCM is typically eight. This is done for practical purposes since models with more than eight VOIs are very complex and difficult to interpret.

In the left hemisphere, the inferior occipital region (iOCC) was chosen given its proximity to the lesion in AH and the high probability of involvement in early visual processing of words. The superior occipital region (sOCC) was chosen to test the hypothesis of a more dorsal pathway for reading. Noteworthy was the lack of any overactivation in earlier visual areas (including V1). Homologues for the iOCC and sOCC were selected in the right hemisphere. The right thalamic region was selected to address the hypothesis of the right hemisphere connecting to left hemisphere language areas via a subcortical pathway. The ventral post-central region (p1) was hypothesized to be the output region for reading and hence included in the DCMs. The ventral pre-central (p2) region was selected given that it was the most significantly overactivated cortical region in AH when compared with controls. Finally, given its anatomical location and overactivation, the superior temporal sulcus (STS) region was selected as a candidate intermediate region between the occipital regions and the pre- and post-central regions.

Controls were selected for a qualitative comparison with patient AH. A more rigorous quantitative comparison could not be achieved given the current limitations of DCM as implemented in SPM 5. In controls, a custom script established seven VOIs per subject using the same contrasts and threshold as AH. Variable distances of up to 6 mm from AH's VOI coordinates were permitted such that largest z-value was obtained for each control. As in AH, a spherical VOI (radius = 4 mm) was then defined and the eigenvector extracted for the given region.

4 Results

4.1 Occipital Regions

A total of four occipital regions were included in a DCM to examine effective connectivity in early visual regions involved in reading.

4.1.1 Occipital Regions in AH

The four occipital regions were investigated in AH. One set of DCMs permitted all forwards and backwards intrinsic and modulatory connections (fully connected). Another set of DCMs barred forwards and backwards cross-connections between inferior and superior regions (disconnected) (Figure 4.1.1). Inputs were then specified to enter the left inferior occipital region, the right inferior occipital region, or bilaterally. This resulted in the fully connected and disconnected DCMs each having three possible forms. The winning model was found to have inputs entering the left iOCC and showed statistically significant forward intrinsic connections from the left iOCC to sOCC and then over to the right sOCC. Note that the threshold for significance for connections here and throughout the study was set at a 95% level of significance. Table 4.1.1 reports Bayes factors for inputs and model comparisons.

DISCONNECTED AND FULLY CONNECTED MODELS FOR FOUR OCCIPITAL REGIONS IN PATIENT AH

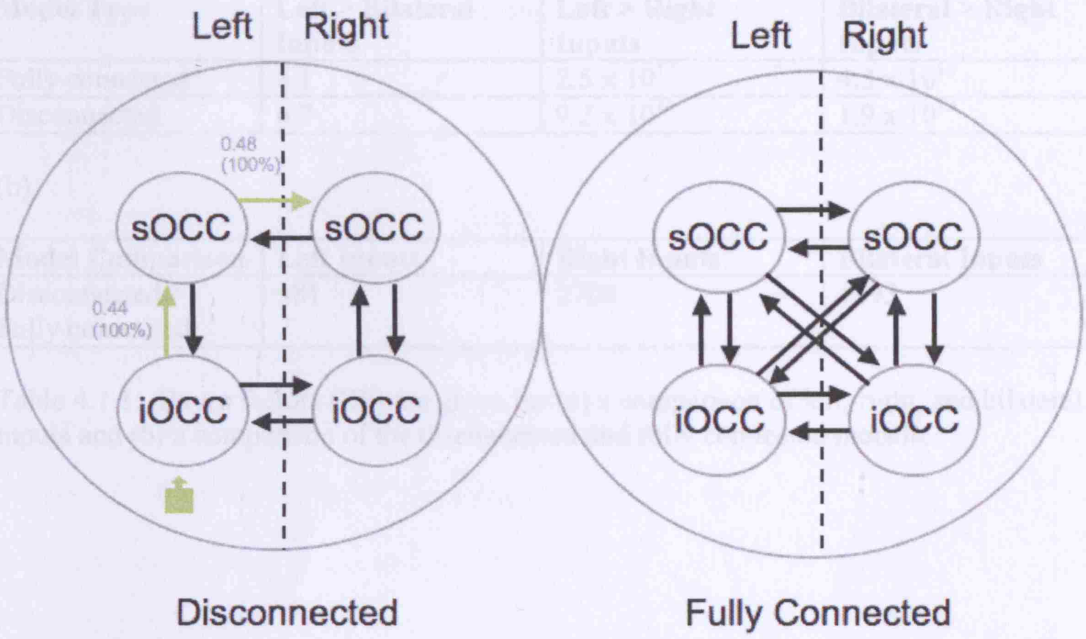

Figure 4.1.1: All permitted intrinsic connections are shown for patient AH. For the disconnected model, statistically significant connections are depicted in green while intrinsic connections lower than a 95% level of significance are in black. When compared with inputs entering the model from the right or bilaterally, inputs entering the left iOCC consistently showed more evidence in their favor. The disconnected model always had very strong evidence when compared with the fully connected model (Table 4.1.1). Hence intrinsic connections for the fully connected model depicted above are only for illustrative purposes and their values and statistical significance are not reported.

BAYES FACTORS COMPARING FOUR OCCIPITAL REGIONS IN PATIENT AH

(a)

Model Type	**Left > Bilateral Inputs**	**Left > Right Inputs**	**Bilateral > Right Inputs**
Fully connected	8.1	2.5×10^{17}	4.3×10^{13}
Disconnected	6.7	9.2×10^{16}	1.9×10^{13}

(b)

Model Comparison	**Left Inputs**	**Right Inputs**	**Bilateral Inputs**
Disconnected > Fully connected	981	2700	1193

Table 4.1.1: Bayes factors (BF) are given for (a) a comparison of left, right, and bilateral inputs and (b) a comparison of the disconnected and fully connected models.

Aside from the winning model, exceedingly large Bayes factors resulted from comparisons with right hemisphere inputs (Table 4.1.1a). It was thus not surprising that no intrinsic connections were found to be statistically significant when inputs entered right iOCC (Appendix 1). Indeed, according to the criteria set forth by Penny *et al.* (2004), the Bayes factor comparing the disconnected to fully connected model showed very strong evidence in favor of the disconnected model. There was positive evidence in favor of left inputs compared to bilateral inputs in the disconnected model. Although this evidence was not particularly strong, the bilateral input model revealed the same pattern of intrinsic connections as the model with left inputs. These results indicated AH primarily used her left occipital lobe for early visual processing.

4.1.2 Occipital Regions in Controls

The data in controls marked a departure from AH. For both the fully connected and disconnected DCMs with right iOCC inputs, controls showed significant intrinsic connections between all regions, although the number of controls having particular connections varied. Looking at the disconnected model with left inputs (the winning model for AH), 26 out of 27 controls show an interhemispheric left to right iOCC connection not observed in AH while 8 out of 27 controls showed the reverse connection. Thus, controls showed greater connectivity when compared with AH, especially between inferior occipital regions.

4.2 Dorsal vs. Ventral Pathway

Given that AH primarily used her left occipital lobe for early visual processing during reading, the hypotheses of an alternative dorsal or ventral pathway for reading were investigated.

4.2.1 Dorsal vs. Ventral Pathway in AH

A comparison of driving inputs was conducted to test the competing hypotheses of a dorsal or ventral pathway for reading. A DCM was initially specified in which the p1, p2, STS, iOCC, and sOCC regions in the left hemisphere had all possible connections (fully connected). Driving inputs were defined to enter the left iOCC in order to model a ventral reading pathway. A second fully connected model was specified in which inputs entered the left sOCC in order to model a dorsal reading pathway (Figure 4.2.1.1). Comparison of the two models indicated strong evidence in favor of iOCC inputs (BF = 103.5). This provided the first evidence of an alternative ventral reading pathway within the left hemisphere.

COMPARISON OF INFERIOR AND SUPERIOR OCCIPITAL INPUTS FOR THE FULLY CONNECTED LEFT HEMISPHERE MODEL IN PATIENT AH

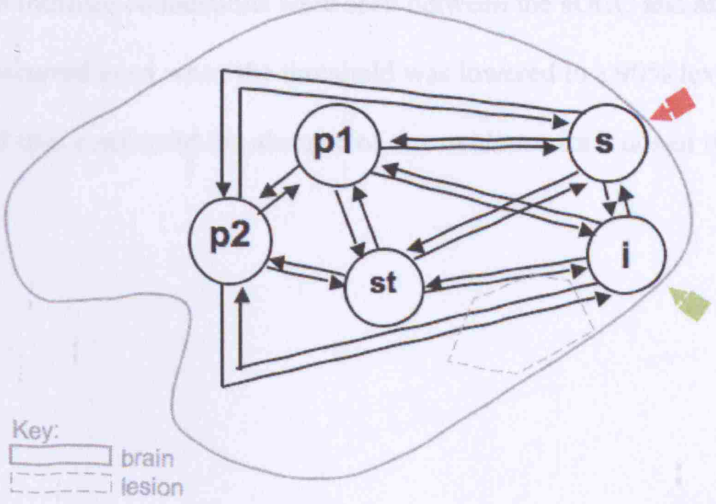

Figure 4.2.1.1: Fully connected left hemisphere DCM in patient AH. Strong evidence was found for inferior inputs (green) over superior inputs (red). In the diagram, 's' refers to the superior occipital region (sOCC), 'i' refers to the inferior occipital region (iOCC), 'st' refers to the superior temporal sulcus (STS), 'p1' refers to the ventral post-central region, and 'p2' refers to the ventral pre-central region.

Building upon the established iOCC input region, the effective connectivity in AH was computed. Figure 4.2.1.2 illustrates the significant effective connectivity in AH. Interestingly, no intrinsic connections were seen between the sOCC and any other regions. This occurred even when the threshold was lowered to a 90% level of significance and thus confirmed the absence of any evidence for a dorsal reading pathway in AH.

FULLY CONNECTED LEFT HEMISPHERE MODEL

WITH INFERIOR INPUTS IN PATIENT AH

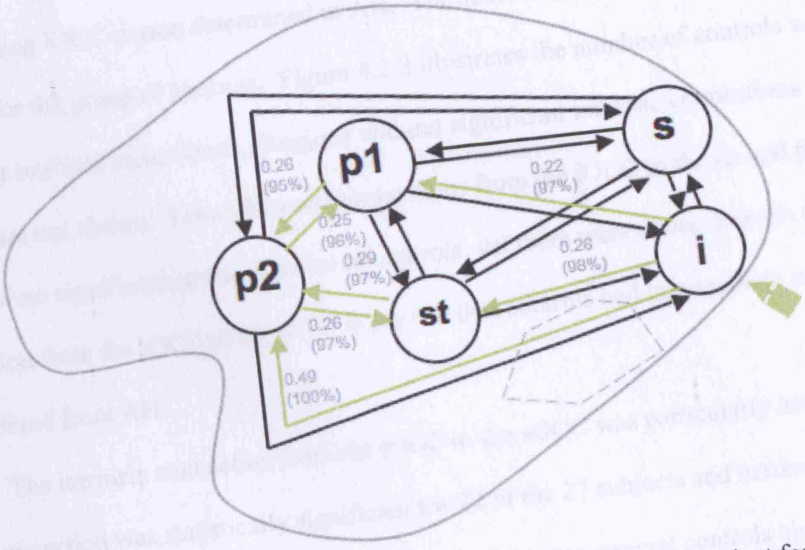

Figure 4.2.1.2: Statistically significant intrinsic connections (green) project forward from the inferior occipital region. Intrinsic connections lower than a 95% level of significance are shown in black. Note the lack of connectivity with the superior occipital region.

4.2.2 Dorsal vs. Ventral Pathway in Controls

Given the controls served as a comparison with AH, the inputs were defined to be in the winning iOCC region determined in AH. The same fully connected DCM was then specified for the group of controls. Figure 4.2.2 illustrates the number of controls with significant intrinsic connections. Regions without significant intrinsic connections in controls are not shown. Direct forward connections from the iOCC to the p1 and p2 regions were significant in the majority of controls, yet there were fewer controls with a connection from the iOCC to the STS. It may be that controls had intermediate regions that differed from AH.

The intrinsic connection from the iOCC to the sOCC was particularly noteworthy. This connection was statistically significant for 22 of the 27 subjects and marked a clear difference from the case of AH. As Figure 4.2.2 illustrates, several controls also differed from AH by exhibiting significant intrinsic connectivity between the sOCC and p1. However, of the five subjects who, like AH, did not show any significant intrinsic connection with the sOCC, only one subject had a backward connection from the STS to the iOCC. Unlike AH, none of the aforementioned five controls had significant forward or backward intrinsic connections between the STS, p1, and p2 regions. Thus, controls that appeared to have a ventral reading pathway on the basis of an iOCC to STS connection and absence of connections with the sOCC did not show intrinsic connections with more anterior regions. There was thus no evidence for controls using the same ventral pathway that was used by AH. A large number (22) of controls showed evidence of a more dorsal reading pathway. Such a pathway may rely on intermediate regions not included in the current DCM.

FULLY CONNECTED LEFT HEMISPHERE MODEL

WITH INFERIOR INPUTS IN CONTROLS

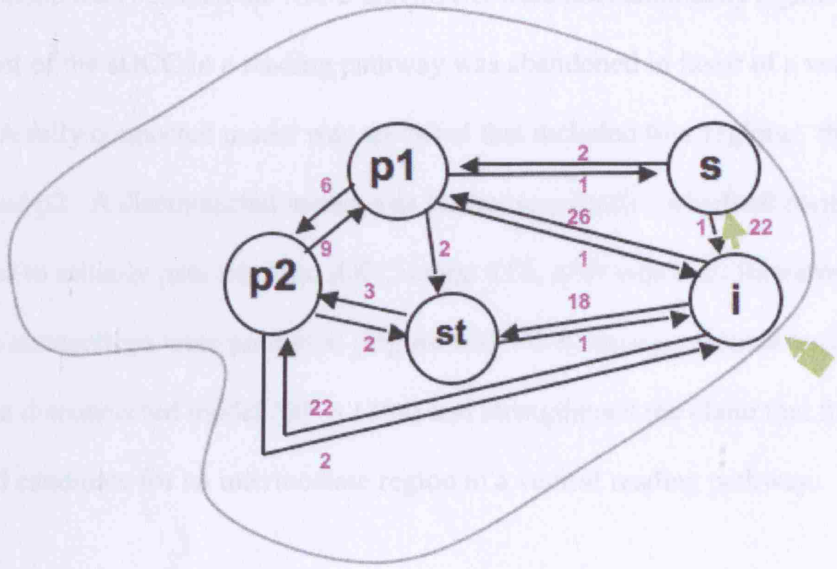

Figure 4.2.2: Pink values indicate the number of controls, out of 27, with intrinsic connections (black) reaching a 95% level of significance. Intrinsic connections are not shown when no controls had a given intrinsic connection at a 95% level of significance. Note the large number of controls with an intrinsic connection from the inferior to superior occipital region (green).

4.3 Fully Connected vs. Disconnected Ventral Pathway in AH

Returning to AH, since there was strong evidence in favor of iOCC inputs and the intrinsic connections between the iOCC and sOCC were not statistically significant, involvement of the sOCC in a reading pathway was abandoned in favor of a ventral pathway. A fully connected model was specified that included four regions: the iOCC, STS, p1, and p2. A disconnected model was further specified in which all connections were forced to initially pass from the iOCC to the STS, after which all forwards and backwards connections were permitted (Figure 4.3). Very strong evidence was found in favor of the disconnected model (BF = 1384) and strengthened the claim that the STS was a good candidate for an intermediate region in a ventral reading pathway.

COMPARISON OF DISCONNECTED AND FULLY CONNECTED LEFT HEMISPHERE MODELS IN PATIENT AH

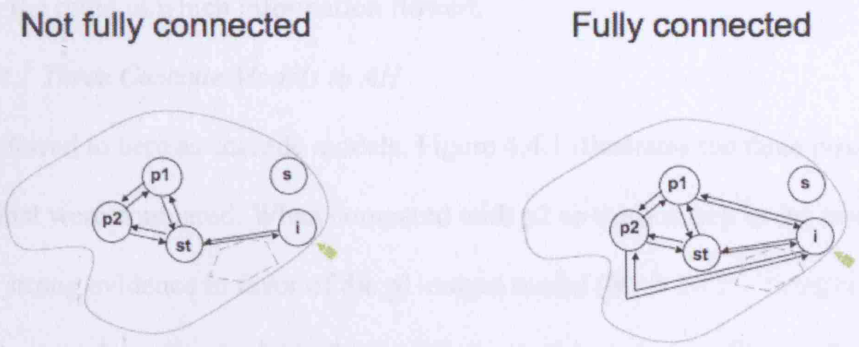

Figure 4.3: Very strong evidence was found in favor of the disconnected model over the fully connected model in AH. The superior occipital region was purposefully excluded from the model given the lack of significant intrinsic connectivity with this region as shown in Figure 4.2.1.2.

4.4 Three Cascade Models

Having established the disconnected model, three models were defined to determine the route in which information flowed.

4.4.1 Three Cascade Models in AH

Referred to here as cascade models, Figure 4.4.1 illustrates the three possible cascades that were compared. When compared with p2 as the last step in the cascade, there was strong evidence in favor of the p1-output model (BF = 20.7). Comparison of the p1-output model to the model including all connections between the p1, p2, and STS again resulted in strong evidence in favor of the p1-output model (BF = 71.1). Finally, a comparison of the p2-output model to the model including all p1, p2, and STS connections yielded positive evidence in favor of the p2-output model (BF = 3.4). Overall, the greatest evidence was found in favor of the model with the p1 region as the last step in the cascade. Interestingly, the values for forward intrinsic connections were roughly twice that of backward intrinsic connections. Overall, the effective connectivity in the ventral reading pathway was refined with the comparison of the three cascade models.

COMPARISON OF THREE LEFT HEMISPHERE CASCADE MODELS

IN PATIENT AH

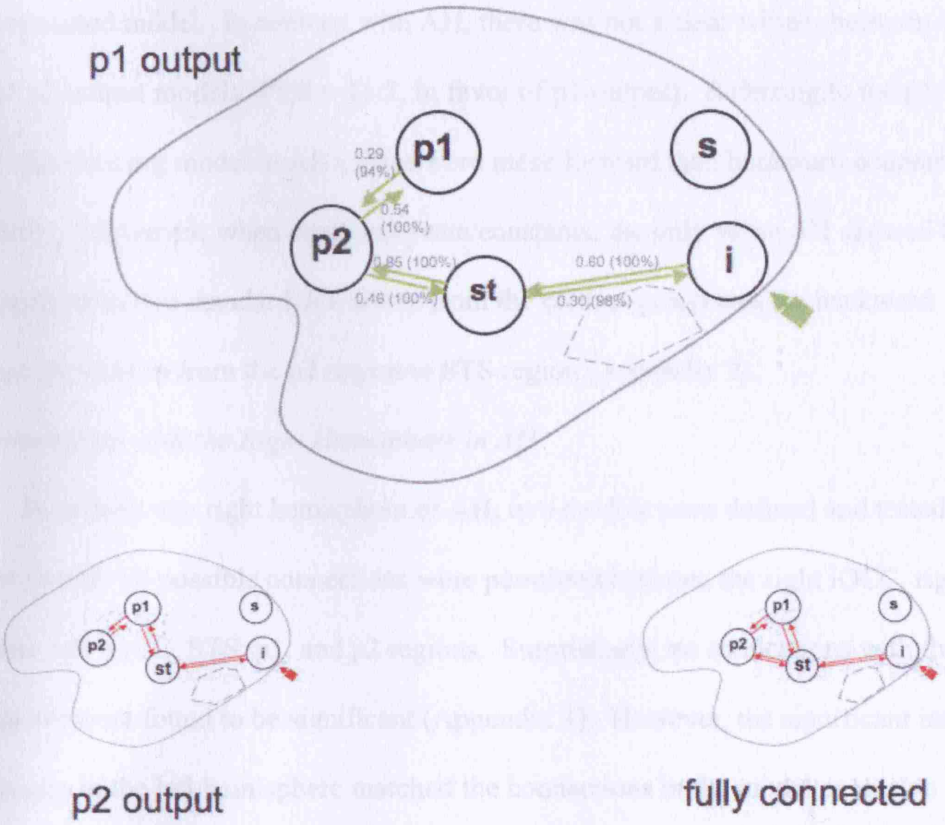

Figure 4.4.1: The model with the ventral post-central region as the end point of the cascade (p1 output) was the overall winner. There was strong evidence in favor of the p1-output model when compared to both the p2-output and fully connected models. Positive evidence was found in favor of the p2-output model when compared with the fully connected model.

4.4.2 Three Cascade Models in Controls

In the majority of controls, the p1-output (PER = 20:1) and p2-output (PER = 19:0) models had positive (or greater) evidence in their favor when compared with the fully connected model. In contrast with AH, there was not a clear winner between the p1- and p2-output models (PER = 11:7, in favor of p1-output). Referring to the p1-output model (the winning model in AH), there were more forward than backward connections in controls. Moreover, when comparing rate constants, the only value AH showed that was greater than two standard deviations from the control group was the backward intrinsic connection from the p2 region to STS region (Appendix 2).

4.5 Connections with the Right Hemisphere in AH

To address the right hemisphere of AH, two models were defined and tested. In the first model, all possible connections were permitted between the right iOCC, right thalamus, left iOCC, STS, p1, and p2 regions. Surprisingly, no connections with the right hemisphere were found to be significant (Appendix 1). However, the significant intrinsic connections in the left hemisphere matched the connections in the model exclusive to the left hemisphere (Figure 4.2.1.2).

Given the p1-output model was the winning model when exclusively considering AH's left hemisphere, this model was connected to right hemisphere regions as well. Since previous evidence favored p1 and not p2 as the output region, it was decided that the right hemisphere regions would connect to the left superior temporal region and p2 (Figure 4.5). Again, no significant intrinsic connections with the right hemisphere were found. Nevertheless, the same p1-output model found when solely modeling the left hemisphere (Figure 4.4.1) was found in the current bilateral DCM.

MODEL CONNECTING THE LEFT AND RIGHT HEMISPHERES IN PATIENT AH

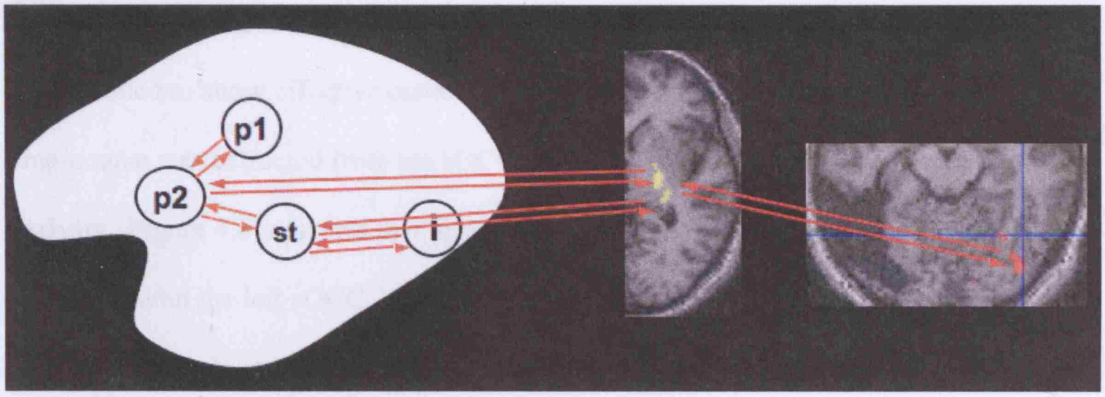

Figure 4.5: Bilateral inputs were specified for patient AH. The right inferior occipital region (far right) was modeled with forwards and backwards intrinsic connections to the thalamus (middle) which then project to the superior temporal sulcus and ventral pre-central regions (far left). The regions chosen preserved the established p1-output model while permitting connections with between regions likely to receive interhemispheric connections. Note that a fully connected model was also permitted in which all forwards and backwards connections between all left and right hemisphere regions were also estimated.

4.6 Accounting for the Superior Occipital Region

Finally, the paradox AH exhibited in showing activation of the left sOCC while DCMs failed to show effective connectivity with the left sOCC was investigated. The time-course was extracted from the sOCC and compared to other regions in a covariance analysis. Figure 4.6 indicates that, in addition to the right hemisphere homologue covarying with the left sOCC, bilateral covariance was seen in the parietal lobe. This suggested a top-down mechanism, such as attention, producing the overactivation in AH's sOCC.

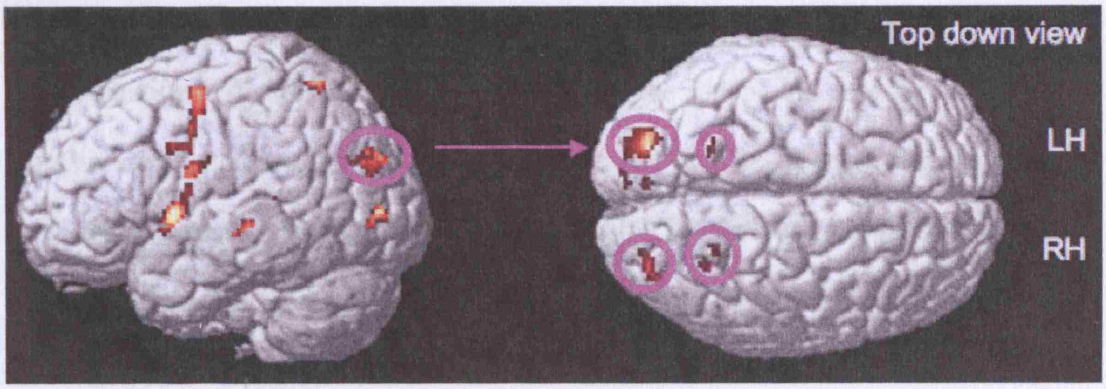

Figure 4.6: Regions in which AH overactivated above controls during reading are shown on the left. Given the lack of evidence for inclusion of the left superior occipital region (sOCC) in DCMs, a covariance analysis was performed. Covariance of the left sOCC with the right hemisphere homologue and bilateral parietal regions is shown on the right.

5 Discussion

The read word has revealed much about AH's residual reading ability. However, it is instructive to first recall how AH reads. While the patient was able to read single words correctly, there was a strong word length effect such that longer words have longer mean reaction times. This slow pace is consistent yet too fast for a serial reading strategy. Given that the patient was able to read correctly, perceptual processing of words can be concluded to be intact.

The results from the four occipital regions confirmed AH primarily used her left occipital lobe for early visual processing. Further, a previous comparison of AH to controls yielded underactivation in a neighboring inferior occipital region (-30 -90 -8). In contrast, the inferior occipital region investigated here (-30 -86 2) yielded overactivation when compared to controls. The proximity of the two regions suggests they may share function. Given that the underactivated region was damaged during AH's stroke, it is possible that a neighboring region took over the damaged region's function. AH's ability to see words without difficulty supports this claim. Alternatively, the overactivated region may be a degenerate system. It cannot be determined at this stage whether the iOCC activation was due to plasticity or the unveiling of a degenerate system.

5.1 The Dorsal Pathway Hypothesis

The strong evidence in favor of inferior occipital inputs provided a fresh view of the activation patterns in AH. Given the overactivation of this region relative to controls and the aforementioned underactivated inferior occipital region, it was hypothesized that the superior occipital region drove the remainder of the compensatory system in AH during reading. However, DCM analyses suggested that the superior occipital region was

not directly involved in reading. Evidence for this came from the favored inferior inputs and the lack of intrinsic connections with the sOCC region (Figure 4.2.1.2). Rather, as the covariance analysis suggests, the overactivation in the superior occipital region was likely due to a top-down mechanism, such as attention, that is necessary but not sufficient for AH to read.

Overactivation of the superior occipital region in AH was particularly curious given 22 out of 27 controls showed significant intrinsic connections between the inferior and superior occipital regions. Supposing that the superior region was part of a top-down network and the inferior region part of a bottom-up network, it follows from the covariance analysis and DCMs that AH dissociated the two networks while the networks remained associated in controls. Yet, the answer cannot be this straightforward since five controls did not show significant intrinsic connectivity between the two occipital regions. It therefore seems unlikely that the lesion in AH disconnected two networks, although the data may be indicative of different strategies when reading. This is not surprising though, since words cause an attentional focus (Reichle *et al.*, 2008) and AH may have required increased vigilance. Thus the comparison of iOCC and sOCC inputs and intrinsic connectivity pattern AH displayed, along with the sOCC covariance analysis, permits the rejection of the hypothesis that AH uses a dorsal pathway for reading.

5.2 The Ventral Pathway Hypothesis

Despite evidence against the dorsal pathway hypothesis, several results supported the hypothesis of an alternative ventral pathway. Returning to the fully connected left-hemisphere model in AH (Figure 4.2.1.2), a clear pathway from the iOCC to the post-central gyrus via an intermediate region was found. This was refined to the point of

establishing and testing the three cascade models (Figure 4.4.1). Given that these regions were overactivated in the patient when compared to controls, it would appear that AH is using an alternative ventral pathway for reading. However, controls needed to be taken into account.

Returning to the fully connected left-hemisphere model in controls (Figure 4.2.2), several subjects were seen to include intrinsic connections that were different from AH. Aside from the 22 controls showing the iOCC to sOCC intrinsic connection mentioned in Section 5.1, it could be supposed that the five subjects not showing the significant intrinsic connection were more similar to AH. In contrast with the fully connected left-hemisphere model in AH, the five controls thought to be similar to AH had no forward connections from the iOCC to STS. Only one subject had a backward connection from the STS region to the iOCC. Moreover, none of the five controls had any significant forward or backward intrinsic connections between the STS region and pre-motor regions. Thus among the subgroup of controls, DCM analysis revealed that they were not similar to AH. In sum, AH differs from controls in terms of local intrinsic connections within the fully connected model.

When forcing controls into the three cascade models tested in AH (Figure 4.2.2), evidence weighed against the fully connected model, yet clear evidence in favor of either the p1- or p2-output model could not be established. This occurred despite the p1-output model being the clear winner for AH. In the absence of clear evidence for a winning output model in controls, no comparison for winning output models between AH and controls can be made.

5.3 The Interhemispheric Hypothesis

Finally, according to Cohen *et al.* (2003), the right VWFA would be expected to take over the damaged left VWFA function. As outlined previously, the right VWFA area was not activated in AH. There was, however, a right inferior occipital region that was posterior to the right VWFA and showed overactivation. Further, a thalamic region showed overactivation when compared with controls. Including these two right hemisphere regions in a fully connected model with the left hemisphere failed to show any involvement in a reading network. Further, when connecting the right occipital and thalamic regions to the p1-output model in the left hemisphere, there were no intrinsic connections with the two right hemisphere regions. Thus, the evidence from the current experiment argues against the hypothesis that the non-VWFA right occipital region connected with the left hemisphere via a subcortical region.

5.4 Revisiting the Cohen Model

The data from previous fMRI studies and the current DCM analyses indicate the Cohen model requires modification. Specifically, the current study suggests that damage to the left occipito-temporal region does not necessarily result in right hemisphere compensation. Rather, there appears to be an alternative ventral pathway, as seen in AH, involved in reading and connecting the inferior occipital cortex, STS, as well as pre- and post-central regions. This study marks the first DCM analysis of an alexic. As such, replication of the findings in other alexics is needed. However, within AH, the data was replicated such that the same winning DCMs were statistically significant when the left hemisphere was modeled by itself or along with two right hemisphere regions.

The qualitative comparison of AH's DCMs to those of controls indicated a high degree of heterogeneity within the normal population. Thus individual differences need consideration when studying reading pathways in health and disease. As such, the Cohen model has been useful in providing a framework for interpreting reading strategies yet simplistic in its explanatory power.

5.5 Technical Discussion

The clear advantage of using DCM in the current study was the ability to clarify the dynamic of activation patterns during reading. This permitted more precise hypotheses about reading and its processing in AH and controls at the local level (i.e. for a given connection). The clear disadvantage of DCM was the qualitative comparison with controls. Given the recent addition of DCM to the neuroimaging toolkit, more robust comparisons of single subjects to group data have yet to materialize.

No matter which VOIs were specified, the complexity of models (and the difficulty in interpretation) increased with every additional VOI or connection. Thus, there always remained a possibility that the DCMs did not include all regions involved in reading. In controls, only a subset (27 out of 47) of neurologically normal subjects showed significant activation ($p < 0.05$) within 6 mm of the regions activated in AH. This indicated heterogeneity within the controls before DCMs were defined. Of the 27 controls with activation near the regions in AH, the variable radius allowed for the highest z-value to be obtained. However, this also permitted the VOI to wander from the intended target and introduced experimental error. Given that all comparisons using DCM between AH and controls were necessarily qualitative, this source of variability was negligible, although it may add variability in the DCMs AH was compared with.

The amount of error this method added is likely to be minimal though, given that images were smoothed with a 6 mm kernel and the 4 mm radius of the spherical VOI would include signal in a VOI at the original coordinates.

It is possible that the thalamic VOI, while showing a high z-value, was not relevant for AH's residual reading ability. This VOI may have been a false positive due to its anatomical location (i.e. it may correspond to white matter). Motion artifact may have also resulted in the observed signal. However, this possibility did not greatly diminish the conclusion to reject the hypothesis that the right iOCC connected to the left hemisphere since a fully connected model allowed the right iOCC to connect with all left hemisphere VOIs. However, it diminishes the evidence for right iOCC connections to the left hemisphere via a subcortical pathway.

The lack of power for single subject statistical analyses did not permit significant modulatory connections for AH (Appendix 1). Yet notably, at the group level, modulatory connections were significant for controls (Appendix 2). This effect was likely due to a low signal-to-noise ratio (SNR) in the time series and at present there was no way of mitigating such an effect. Hence only intrinsic connections in AH were compared with intrinsic connections in controls.

A word on interpreting intrinsic connections is also warranted. It will be recalled that VOIs were selected on the basis of AH overactivating during reading when compared to controls. However, when the eigenvectors were extracted from these regions, all four tasks (Section 3.4) were used as inputs in all DCMs. This was another limitation of DCM in its current state. As such, intrinsic connection values were related to all four tasks while modulatory connections were related to the modulatory effect of

reading on the intrinsic connections. However, given that AH had difficulty when naming objects (Seghier and Price, unpublished), and the third and fourth tasks were baseline conditions, the eigenvectors were likely to be mainly due to reading or pronunciation. Nevertheless, this adds a potential source of error to the current study.

5.6 Future directions

Due to time restrictions and the large number of research questions to be asked of AH, the current study required a narrow scope in order to make the hypotheses and models manageable. Hence, the ventral left hemisphere pathway may be further tested in at least four ways. First, additional intermediate regions between the occipital, pre- and post-central regions may be added to the model to determine if the ventral pathway is the only reading pathway within AH. Second, the right VWFA could undergo a covariance analysis to determine which areas it correlates with. A DCM could then test if these regions form a coherent pathway for reading. Third, the qualitative results between AH and controls suggests that transcranial magnetic stimulation (TMS) of the left sOCC may affect controls more than AH. Attention would have to be directed towards dissecting top-down processes and reading should such an experiment be conducted. Fourth, diffusion tensor imaging (DTI) may corroborate the ventral reading pathway identified by confirming white matter connections between regions identified in the p1-output model.

The final two future directions listed above are particularly important. As Logothetis (2008) points out, a typical unfiltered voxel used in fMRI analyses contains 5.5 million neurons, 22 km of dendrites, and 220 km of axons. This complex neural circuitry within a single voxel may cause one to dismiss fMRI findings. Yet as Logothetis notes, despite the shortcomings of fMRI, it is currently the best tool for

investigating human brain function. Using a multimodal strategy, fMRI findings may be coupled with modalities such as EEG or TMS. The current study refined the functional connectivity observed in previous studies while establishing an alternative ventral pathway for reading. Thus a framework for testing additional hypotheses was established and may inform other studies using other modalities.

Aside from research, the findings on effective connectivity in the neural pathways for reading may be of clinical relevance. As Losseff and Brown (2003) note, stroke patients naturally show a gradual improvement over time unless secondary complications or primary neurological death arise. The goal of rehabilitation is then to boost such spontaneous recovery. However, rehabilitation must be addressed at the levels of impairment, limitation of activity (disability), and limitation of participation (handicap). In pure alexia, rehabilitation involves the main techniques of letter-by-letter reading and turning implicit reading into explicit reading (Behrmann *et al.*, 1990; Greenwald and Gonzalez Rothi, 1998). By mapping critical pathways for reading, more personalized, well informed, and efficient rehabilitation strategies may be discovered and translated into clinical practice. Such strategies impact rehabilitation at the levels of impairment, disability, and handicap by allowing the patient to read more effectively in daily life.

6 Conclusion

The results indicate that patient AH is able to read despite her left occipito-temporal lesion by using a previously unknown ventral pathway. This result does not preclude other regions being involved in reading. However the results do indicate that a lesion to the putative left hemisphere VWFA does not terminate reading function in intact brain regions within the left hemisphere.

7 References

Aertsen, A., & Preißl, H. (1991). Dynamics of activity and connectivity in physiological neuronal Networks. In H. G. Schuster (Ed.), *Non linear dynamics and neuronal networks* (pp. 281-302). New York: VCH Publishers.

Aghababian, V. & Nazir, T. A. (2000). Developing normal reading skills: aspects of the visual processes underlying word recognition. *J.Exp. Child Psychol., 76,* 123-150.

Behrmann, M., Black, S. E., & Bub, D. (1990). The evolution of pure alexia: a longitudinal study of recovery. *Brain Lang., 39,* 405-427.

British Library. (2008). *Facts and Figures*. Retrieved July 20, 2008, from: http://www.bl.uk/aboutus/quickinfo/facts/index.html

Buckner, R. L., Bandettini, P. A., O'Craven, K. M., Savoy, R. L., Petersen, S. E., Raichle, M. E. et al. (1996). Detection of cortical activation during averaged single trials of a cognitive task using functional magnetic resonance imaging. *Proc.Natl.Acad.Sci.U.S.A, 93,* 14878-14883.

Buckner, R. L., Goodman, J., Burock, M., Rotte, M., Koutstaal, W., Schacter, D. et al. (1998). Functional-anatomic correlates of object priming in humans revealed by rapid presentation event-related fMRI. *Neuron, 20,* 285-296.

Cohen, L., Martinaud, O., Lemer, C., Lehericy, S., Samson, Y., Obadia, M. et al. (2003). Visual word recognition in the left and right hemispheres: anatomical and functional correlates of peripheral alexias. *Cereb.Cortex, 13,* 1313-1333.

Dejerine, J. (1891). Sur un cas de cécité verbale avec agraphie suivi d'autopsie. *Mém.Soc.Biol., 3,* 197–201.

Dejerine, J. (1892). Contribution à l'étude anatomo-pathologique et clinique des différentes variétés de cécité verbale. *Mém.Soc.Biol., 4,* 61–90.

Dronkers, N., Pinker, S., & Damsio, A. (2000). Language and the Aphasia. In E.R. Kandel, J. H. Schwartz, and T.M. Jessell (Eds.), *Principles of Neural Science* (4th ed.) (pp. 1169-1186). New York: McGraw-Hill.

Friston, K. J. (1994). Functional and effective connectivity in neuroimaging: a synthesis. *Hum.Brain.Mapping, 2,* 56–78.

Friston, K. J. (2002). Beyond phrenology: what can neuroimaging tell us about distributed circuitry? *Annu.Rev.Neurosci., 25,* 221-250.

Friston, K. J., Harrison, L., & Penny, W. D. (2003). Dynamic causal modelling. *Neuroimage., 19,* 1273-1302.

Friston, K. J. (2007a). Statistical parametric mapping. In K. J. Friston, J. T. Ashburner, S. J. Kiebel, T. E. Nichols, & W. D. Penny (Eds.), *Statistical Parametric Mapping: The Analysis of Functional Brain Images* (pp. 10-31). London: Academic Press.

Friston, K. J. (2007b). Dynamic Causal Models for fMRI. In K. J. Friston, J. T. Ashburner, S. J. Kiebel, T. E. Nichols, & W. D. Penny (Eds.), *Statistical Parametric Mapping: The Analysis of Functional Brain Images* (pp. 541-560). London: Academic Press.

Greenwald, M. L., & Gonzalez Rothi, L. J. (1998). Lexical access via letter naming in a profoundly alexic and anomic patient: a treatment study. *J.Int.Neuropsychol.Soc., 4,* 595–607.

Kass, R. E., & Raftery, A. E. (1995). Bayes factors. *J.Am.Stat.Assoc., 90,* 773– 795.

Lavidor, M. & Ellis, A. W. (2002). Word length and orthographic neighborhood size effects in the left and right cerebral hemispheres. *Brain Lang., 80,* 45-62.

Logothetis, N. K. (2008). What we can do and what we cannot do with fMRI. *Nature, 453,* 869-878.

Losseff, N. A., & Brown, M. M. (2003). Cerebrovascular Disease. In T. J. Fowler and J. W. Scadding (Eds.), *Clinical Neurology* (3rd ed.) (pp. 446-480). London: Arnold.

Morais, J. & Kolinsky, R. (1994). Perception and awareness in phonological processing: the case of the phoneme. *Cognition, 50,* 287-297.

Ogawa, S., Lee, T. M., Kay, A. R., & Tank, D. W. (1990). Brain magnetic resonance imaging with contrast dependent on blood oxygenation. *Proc.Natl.Acad.Sci.U.S.A., 87,* 9868-9872.

Ogawa, S., Menon, R. S., Tank, D. W., Kim, S. G., Merkle, H., Ellermann, J. M., & Ugurbil, K. (1993). Functional brain mapping by blood oxygenation level-dependent contrast magnetic-resonance-imaging: a comparison of signal characteristics with a biophysical model. *Biophys.J., 64,* 803-812.

Penny, W. D., Stephan, K. E., Mechelli, A., & Friston, K. J. (2004). Comparing dynamic causal models. *Neuroimage., 22,* 1157-1172.

Reichle, E. D., Vanyukov, P. M., Laurent, P. A., & Warren, T. (2008). Serial or parallel? Using depth-of-processing to examine attention allocation during reading. *Vision Res., 48,* 1831-1836.

Rosen, B. R., Buckner, R. L., & Dale, A. M. (1998). Event-related functional MRI: past, present, and future. *Proc.Natl.Acad.Sci.U.S.A., 95,* 773-780.

Seghier, M. L., Friston, K. J., & Price, C. J. (2007). Detecting subject-specific activations using fuzzy clustering. *Neuroimage, 36*, 594-605.

Seghier, M. L., Lee, H. L., Schofield, T., Ellis, C. L., & Price, C. J. (2008). Inter-subject variability in the use of two different neuronal networks for reading aloud familiar words. *Neuroimage* (In Press), Epub, May 28, 2008.

Shakespeare, W. (1623). The First Folio. London: Isaac Iaggard and Edward Blount.

Smyser, C., Grabowski, T. J., Frank, R. J., Haller, J. W., & Bolinger, L. (2001). Real-time multiple linear regression for fMRI supported by time-aware acquisition and processing. *Magn.Reson.Med., 45,* 289-298.

Stephan, K. E., Harrison, L. M., Kiebel, S. J., David, O., Penny, W. D., & Friston, K. J. (2007). Dynamic causal models of neural system dynamics:current state and future extensions. *J.Biosci., 32,* 129-144.

Turner, R., Howseman, A., Rees, G. E., Josephs, O., & Friston, K. J. (1998). Functional magnetic resonance imaging of the human brain: data acquisition and analysis. *Exp.Brain.Res., 123*, 5-12.

Weekes, B. S. (1997). Differential effects of number of letters on word and non-word naming latency. *Q.J.Exp.Psychol., 50A*, 439–456.

Weiskopf, N., Hutton, C., Josephs, O., & Deichmann, R. (2006). Optimal EPI parameters for reduction of susceptibility-induced BOLD sensitivity losses: a whole-brain analysis at 3 T and 1.5 T. *Neuroimage, 33,* 493-504.

Appendix 1, Full Matrices for Patient AH

Note that probabilities may be interpreted as percentages.

(a) Left and right hemispheres, 4 occipital regions, not fully connected, left inputs

Intrinsic connections (Hz)

	left iOCC	left sOCC	right sOCC	right iOCC
left iOCC	-1.0000	0.2039	0	0.0601
left sOCC	0.4385	-1.0000	0.1664	0
right sOCC	0	0.4774	-1.0000	0.1373
right iOCC	0.0982	0	0.0916	-1.0000

Probability for intrinsic connections (%)

	left iOCC	left sOCC	right sOCC	right iOCC
left iOCC	NaN	0.8601	NaN	0.6181
left sOCC	0.9996	NaN	0.8073	NaN
right sOCC	NaN	0.9992	NaN	0.7567
right iOCC	0.8280	NaN	0.6861	NaN

Modulatory connections (Hz)

	left iOCC	left sOCC	right sOCC	right iOCC
left iOCC	0	0.0049	0	0.0020
left sOCC	0.2035	0	0.0107	0
right sOCC	0	0.1236	0	0.0441
right iOCC	0.1178	0	0.0376	0

Probability for modulatory connections (%)

	left iOCC	left sOCC	right sOCC	right iOCC
left iOCC	NaN	0.5098	NaN	0.5039
left sOCC	0.8884	NaN	0.5216	NaN
right sOCC	NaN	0.7545	NaN	0.5879
right iOCC	0.7803	NaN	0.5754	NaN

(b) Left and right hemispheres, 4 occipital regions, not fully connected, bilateral inputs

Intrinsic connections (Hz)

	left iOCC	left sOCC	right sOCC	right iOCC
left iOCC	-1.0000	0.2177	0	0.0712
left sOCC	0.4243	-1.0000	0.1610	0
right sOCC	0	0.5135	-1.0000	0.0629
right iOCC	0.2394	0	0.0877	-1.0000

Probability for intrinsic connections (%)

	left iOCC	left sOCC	right sOCC	right iOCC
left iOCC	NaN	0.8755	NaN	0.6399
left sOCC	0.9996	NaN	0.8004	NaN
right sOCC	NaN	0.9997	NaN	0.6316
right iOCC	0.9304	NaN	0.6786	NaN

Modulatory connections (Hz)

	left iOCC	left sOCC	right sOCC	right iOCC
left iOCC	0	0.0054	0	-0.0020
left sOCC	0.1803	0	0.0022	0
right sOCC	0	0.1189	0	0.0437
right iOCC	0.0655	0	0.0240	0

Probability for modulatory connections (%)

	left iOCC	left sOCC	right sOCC	right iOCC
left iOCC	NaN	0.5109	NaN	0.5041
left sOCC	0.8666	NaN	0.5045	NaN
right sOCC	NaN	0.7464	NaN	0.5871
right iOCC	0.6318	NaN	0.5479	NaN

(c) Left hemisphere, fully connected, inferior inputs

Intrinsic connections (Hz)

	iOCC	sOCC	STS	P1	P2
iOCC	-1.0000	0.0563	0.1023	0.0871	0.1633
sOCC	0.1354	-1.0000	0.0916	0.0772	0.1369
STS	0.2610	0.1063	-1.0000	0.1662	0.2587
P1	0.2240	0.0990	0.1711	-1.0000	0.2482
P2	0.4861	0.1659	0.2859	0.2605	-1.0000

Probability for intrinsic connections (%)

	iOCC	sOCC	STS	P1	P2
iOCC	NaN	0.6358	0.7460	0.7118	0.8701
sOCC	0.8791	NaN	0.7272	0.6927	0.8385
STS	0.9783	0.7440	NaN	0.8578	0.9654
P1	0.9652	0.7298	0.8690	NaN	0.9616
P2	0.9998	0.8463	0.9675	0.9521	NaN

Modulatory connections (Hz)

	iOCC	sOCC	STS	P1	P2
iOCC	0	-0.0200	-0.0364	-0.0338	-0.0466
sOCC	0.0779	0	-0.0157	-0.0163	-0.0147
STS	0.0777	0.0120	0	0.0173	0.0313
P1	0.0487	0.0020	0.0030	0	0.0078
P2	0.0961	0.0125	0.0215	0.0166	0

Probability for modulatory connections (%)

	iOCC	sOCC	STS	P1	P2
iOCC	NaN	0.5483	0.5887	0.5819	0.6151
sOCC	0.7166	NaN	0.5394	0.5404	0.5386
STS	0.7044	0.5292	NaN	0.5426	0.5798
P1	0.6371	0.5048	0.5075	NaN	0.5204
P2	0.7399	0.5302	0.5529	0.5406	NaN

(d) Left hemisphere, fully connected, superior inputs

Intrinsic connections (Hz)

	iOCC	sOCC	STS	P1	P2
iOCC	-1.0000	0.3789	0.1497	0.1217	0.2134
sOCC	0.0947	-1.0000	0.1053	0.0752	0.1491
STS	0.1780	0.2972	-1.0000	0.1709	0.2710
P1	0.1720	0.2218	0.1894	-1.0000	0.2563
P2	0.2946	0.4552	0.3222	0.2798	-1.0000

Probability for intrinsic connections (%)

	iOCC	sOCC	STS	P1	P2
iOCC	NaN	0.9957	0.8362	0.7842	0.9332
sOCC	0.7295	NaN	0.7553	0.6874	0.8539
STS	0.8740	0.9798	NaN	0.8651	0.9715
P1	0.8671	0.9418	0.8935	NaN	0.9657
P2	0.9703	0.9989	0.9818	0.9638	NaN

Modulatory connections (Hz)

	iOCC	sOCC	STS	P1	P2
iOCC	0	-0.0629	-0.0588	-0.0521	-0.0764
sOCC	-0.0186	0	-0.0295	-0.0296	-0.0361
STS	0.0101	0.0452	0	0.0107	0.0208
P1	-0.0018	0.0098	-0.0008	0	-0.0002
P2	0.0113	0.0461	0.0189	0.0124	0

Probability for modulatory connections (%)

	iOCC	sOCC	STS	P1	P2
iOCC	NaN	0.6641	0.6449	0.6271	0.6918
sOCC	0.5452	NaN	0.5731	0.5728	0.5916
STS	0.5248	0.6183	NaN	0.5265	0.5540
P1	0.5043	0.5267	0.5020	NaN	0.5005
P2	0.5275	0.6189	0.5472	0.5307	NaN

(e) Left hemisphere, no sOCC, fully connected, inferior inputs

Intrinsic connections (Hz)

	iOCC	STS	P1	P2
iOCC	-1.0000	0.1366	0.1057	0.2113
STS	0.2800	-1.0000	0.1952	0.3174
P1	0.2108	0.2075	-1.0000	0.2920
P2	0.5304	0.3840	0.3298	-1.0000

Probability for intrinsic connections (%)

	iOCC	STS	P1	P2
iOCC	NaN	0.7741	0.7163	0.9008
STS	0.9620	NaN	0.8548	0.9745
P1	0.9190	0.8757	NaN	0.9655
P2	0.9993	0.9827	0.9624	NaN

Modulatory connections (Hz)

	iOCC	STS	P1	P2
iOCC	0	-0.0367	-0.0340	-0.0445
STS	0.1043	0	0.0302	0.0552
P1	0.0670	0.0147	0	0.0241
P2	0.1150	0.0431	0.0323	0

Probability for modulatory connections (%)

	iOCC	STS	P1	P2
iOCC	NaN	0.5757	0.5694	0.5948
STS	0.7204	NaN	0.5621	0.6196
P1	0.6506	0.5311	NaN	0.5538
P2	0.7351	0.5890	0.5660	NaN

(f) Left hemisphere, no sOCC, not fully connected, inferior inputs (same as fully connected cascade)

Intrinsic connections (Hz)

	iOCC	STS	P1	P2
iOCC	-1.0000	0.2819	0	0
STS	0.5635	-1.0000	0.2263	0.3439
P1	0	0.4111	-1.0000	0.2841
P2	0	0.7094	0.3718	-1.0000

Probability for intrinsic connections (%)

	iOCC	STS	P1	P2
iOCC	NaN	0.9732	NaN	NaN
STS	0.9999	NaN	0.8975	0.9864
P1	NaN	0.9958	NaN	0.9620
P2	NaN	1.0000	0.9790	NaN

Modulatory connections (Hz)

	iOCC	STS	P1	P2
iOCC	0	-0.0612	0	0
STS	0.1962	0	0.0077	0.0175
P1	0	0.0448	0	-0.0073
P2	0	0.0770	0.0065	0

Probability for modulatory connections (%)

	iOCC	STS	P1	P2
iOCC	NaN	0.6310	NaN	NaN
STS	0.8640	NaN	0.5161	0.5390
P1	NaN	0.6050	NaN	0.5162
P2	NaN	0.6688	0.5135	NaN

(g) Left hemisphere, p2-output

Intrinsic connections (Hz)

	iOCC	STS	P1	P2
iOCC	-1.0000	0.3374	0	0
STS	0.5794	-1.0000	0.4157	0
P1	0	0.7557	-1.0000	0.2885
P2	0	0	0.8265	-1.0000

Probability for intrinsic connections (%)

	iOCC	STS	P1	P2
iOCC	NaN	0.9862	NaN	NaN
STS	0.9999	NaN	0.9982	NaN
P1	NaN	1.0000	NaN	0.9626
P2	NaN	NaN	1.0000	NaN

Modulatory connections (Hz)

	iOCC	STS	P1	P2
iOCC	0	-0.0593	0	0
STS	0.1920	0	0.0172	0
P1	0	0.0947	0	-0.0312
P2	0	0	0.0593	0

Probability for modulatory connections (%)

	iOCC	STS	P1	P2
iOCC	NaN	0.6264	NaN	NaN
STS	0.8615	NaN	0.5390	NaN
P1	NaN	0.7142	NaN	0.5670
P2	NaN	NaN	0.6298	NaN

(h) Left hemisphere, p1-output

Intrinsic connections (Hz)

	iOCC	STS	P1	P2
iOCC	-1.0000	0.3042	0	0
STS	0.5955	-1.0000	0	0.4649
P1	0	0	-1.0000	0.5390
P2	0	0.8543	0.2858	-1.0000

Probability for intrinsic connections (%)

	iOCC	STS	P1	P2
iOCC	NaN	0.9833	NaN	NaN
STS	1.0000	NaN	NaN	0.9997
P1	NaN	NaN	NaN	1.0000
P2	NaN	1.0000	0.9405	NaN

Modulatory connections (Hz)

	iOCC	STS	P1	P2
iOCC	0	-0.0702	0	0
STS	0.1989	0	0	0.0245
P1	0	0	0	0.0240
P2	0	0.1022	-0.0126	0

Probability for modulatory connections (%)

	iOCC	STS	P1	P2
iOCC	NaN	0.6515	NaN	NaN
STS	0.8675	NaN	NaN	0.5577
P1	NaN	NaN	NaN	0.5615
P2	NaN	0.7262	0.5259	NaN

(i) Left and right hemispheres, fully connected, bilateral inputs

Intrinsic connections (Hz)

	liOCC	lSTS	lP1	lP2	riOCC	rTha
liOCC	-1.0000	0.0838	0.0775	0.1274	0.0263	0.0322
lSTS	0.2516	-1.0000	0.1479	0.2164	0.0485	0.0549
lP1	0.2380	0.1468	-1.0000	0.2106	0.0575	0.0523
lP2	0.4588	0.2257	0.2141	-1.0000	0.0278	0.0747
riOCC	0.1145	0.0198	0.0136	0.0342	-1.0000	0.0212
rTha	0.0787	0.0259	0.0165	0.0379	0.0428	-1.0000

Probability for intrinsic connections (%)

	liOCC	lSTS	lP1	lP2	riOCC	rTha
liOCC	NaN	0.7322	0.7160	0.8361	0.5740	0.5903
lSTS	0.9914	NaN	0.8644	0.9568	0.6357	0.6516
lP1	0.9909	0.8656	NaN	0.9547	0.6604	0.6449
lP2	1.0000	0.9526	0.9427	NaN	0.5786	0.7019
riOCC	0.8262	0.5603	0.5410	0.6116	NaN	0.5598
rTha	0.8424	0.5798	0.5506	0.6263	0.6240	NaN

Modulatory connections (Hz)

	liOCC	lSTS	lP1	lP2	riOCC	rTha
liOCC	0	-0.0046	-0.0046	-0.0050	-0.0020	-0.0016
lSTS	0.0716	0	0.0212	0.0337	0.0086	0.0106
lP1	0.0496	0.0085	0	0.0142	0.0033	0.0048
lP2	0.0897	0.0230	0.0201	0	0.0086	0.0111
riOCC	0.0394	0.0154	0.0131	0.0227	0	0.0087
rTha	0.0577	0.0407	0.0369	0.0554	0.0151	0

Probability for modulatory connections (%)

	liOCC	lSTS	lP1	lP2	riOCC	rTha
liOCC	NaN	0.5131	0.5130	0.5142	0.5057	0.5045
lSTS	0.7205	NaN	0.5604	0.5977	0.5243	0.5300
lP1	0.6640	0.5245	NaN	0.5419	0.5094	0.5135
lP2	0.7597	0.5654	0.5572	NaN	0.5244	0.5314
riOCC	0.6131	0.5439	0.5373	0.5656	NaN	0.5246
rTha	0.7096	0.6173	0.6058	0.6630	0.5427	NaN

(j) Left and right hemispheres, cascade + right hemi, bilateral inputs

Intrinsic connections (Hz)

	liOCC	lSTS	lP1	lP2	riOCC	rTha
liOCC	-1.0000	0.2233	0	0	0	0
lSTS	0.5433	-1.0000	0	0.3918	0	0.0994
lP1	0	0	-1.0000	0.4880	0	0
lP2	0	0.7431	0.2291	-1.0000	0	0.1406
riOCC	0	0	0	0	-1.0000	0.0821
rTha	0	0.1375	0	0.0721	0.0322	-1.0000

Probability for intrinsic connections (%)

	liOCC	lSTS	lP1	lP2	riOCC	rTha
liOCC	NaN	0.9649	NaN	NaN	NaN	NaN
lSTS	1.0000	NaN	NaN	0.9996	NaN	0.7607
lP1	NaN	NaN	NaN	1.0000	NaN	NaN
lP2	NaN	1.0000	0.9547	NaN	NaN	0.8417
riOCC	NaN	NaN	NaN	NaN	NaN	0.7288
rTha	NaN	0.9182	NaN	0.7479	0.5920	NaN

Modulatory connections (Hz)

	liOCC	lSTS	lP1	lP2	riOCC	rTha
liOCC	0	-0.0217	0	0	0	0
lSTS	0.1696	0	0	0.0425	0	0.0129
lP1	0	0	0	0.0451	0	0
lP2	0	0.1068	0.0079	0	0	0.0157
riOCC	0	0	0	0	0	0.0206
rTha	0	0.0602	0	0.0514	0.0041	0

Probability for modulatory connections (%)

	liOCC	lSTS	lP1	lP2	riOCC	rTha
liOCC	NaN	0.5631	NaN	NaN	NaN	NaN
lSTS	0.9101	NaN	NaN	0.6254	NaN	0.5365
lP1	NaN	NaN	NaN	0.6423	NaN	NaN
lP2	NaN	0.8003	0.5226	NaN	NaN	0.5445
riOCC	NaN	NaN	NaN	NaN	NaN	0.5582
rTha	NaN	0.7008	NaN	0.6579	0.5117	NaN

Appendix 2, Full Matrices for Controls

Note that probabilities may be interpreted as percentages. However, at the group level for modulatory connections, probabilities are given as p-values.

(a) Left and right hemispheres, 4 occipital regions, not fully connected, left inputs

Intrinsic connections (Hz)

	left iOCC	left sOCC	right sOCC	right iOCC
left iOCC	-1.0000	0.2411	0	0.1889
left sOCC	0.4752	-1.0000	0.1516	0
right sOCC	0	0.3183	-1.0000	0.2421
right iOCC	0.3695	0	0.0993	-1.0000

Probability for intrinsic connections (p-value)

	left iOCC	left sOCC	right sOCC	right iOCC
left iOCC	NaN	1.0000	NaN	1.0000
left sOCC	1.0000	NaN	1.0000	NaN
right sOCC	NaN	1.0000	NaN	1.0000
right iOCC	1.0000	NaN	1.0000	NaN

Variance for intrinsic connections (Hz^2)

	left iOCC	left sOCC	right sOCC	right iOCC
left iOCC	0	0.0143	0	0.0305
left sOCC	0.0173	0	0.0134	0
right sOCC	0	0.0220	0	0.0356
right iOCC	0.0608	0	0.0084	0

Number of controls with intrinsic connections at a significance of 95% or greater

	left iOCC	left sOCC	right sOCC	right iOCC
left iOCC	0	6	0	8
left sOCC	26	0	2	0
right sOCC	0	16	0	15
right iOCC	26	0	1	0

Modulatory connections (Hz)

	left iOCC	left sOCC	right sOCC	right iOCC
left iOCC	0	-0.0529	0	-0.0440
left sOCC	-0.1063	0	-0.0544	0
right sOCC	0	-0.0026	0	0.0076
right iOCC	-0.0687	0	-0.0310	0

Probability for modulatory connections (p-value)

	left iOCC	left sOCC	right sOCC	right iOCC
left iOCC	NaN	0.0000	NaN	0.0002
left sOCC	0.0000	NaN	0.0000	NaN
right sOCC	NaN	0.4187	NaN	0.6887
right iOCC	0.0072	NaN	0.0001	NaN

Variance for modulatory connections (Hz^2)

	left iOCC	left sOCC	right sOCC	right iOCC
left iOCC	0	0.0031	0	0.0032
left sOCC	0.0114	0	0.0024	0
right sOCC	0	0.0043	0	0.0062
right iOCC	0.0186	0	0.0015	0

Number of controls with modulatory connections at a significance of 95% or greater

	left iOCC	left sOCC	right sOCC	right iOCC
left iOCC	0	0	0	0
left sOCC	3	0	0	0
right sOCC	0	0	0	0
right iOCC	4	0	0	0

(b) Left and right hemispheres, 4 occipital regions, bilateral inputs

Intrinsic connections (Hz)

	left iOCC	left sOCC	right sOCC	right iOCC
left iOCC	-1.0000	0.2257	0	0.1940
left sOCC	0.4668	-1.0000	0.1787	0
right sOCC	0	0.2626	-1.0000	0.2859
right iOCC	0.2324	0	0.0993	-1.0000

Probability for intrinsic connections (p-value)

	left iOCC	left sOCC	right sOCC	right iOCC
left iOCC	NaN	1.0000	NaN	1.0000
left sOCC	1.0000	NaN	1.0000	NaN
right sOCC	NaN	1.0000	NaN	1.0000
right iOCC	1.0000	NaN	1.0000	NaN

Variance for intrinsic connections (Hz^2)

	left iOCC	left sOCC	right sOCC	right iOCC
left iOCC	0	0.0182	0	0.0320
left sOCC	0.0213	0	0.0263	0
right sOCC	0	0.0212	0	0.0552
right iOCC	0.0272	0	0.0103	0

Number of controls with intrinsic connections at a significance of 95% or greater

	left iOCC	left sOCC	right sOCC	right iOCC
left iOCC	0	5	0	9
left sOCC	25	0	4	0
right sOCC	0	12	0	19
right iOCC	13	0	1	0

Modulatory connections (Hz)

	left iOCC	left sOCC	right sOCC	right iOCC
left iOCC	0	-0.0542	0	-0.0332
left sOCC	-0.0998	0	-0.0518	0
right sOCC	0	-0.0071	0	0.0076
right iOCC	-0.0403	0	-0.0288	0

Probability for modulatory connections (p-value)

	left iOCC	left sOCC	right sOCC	right iOCC
left iOCC	NaN	0.0000	NaN	0.0007
left sOCC	0.0000	NaN	0.0000	NaN
right sOCC	NaN	0.2374	NaN	0.6834
right iOCC	0.0003	NaN	0.0002	NaN

Variance for modulatory connections (Hz^2)

	left iOCC	left sOCC	right sOCC	right iOCC
left iOCC	0	0.0032	0	0.0024
left sOCC	0.0085	0	0.0024	0
right sOCC	0	0.0026	0	0.0067
right iOCC	0.0028	0	0.0014	0

Number of controls with modulatory connections at a significance of 95% or greater

	left iOCC	left sOCC	right sOCC	right iOCC
left iOCC	0	0	0	0
left sOCC	2	0	0	0
right sOCC	0	0	0	0
right iOCC	0	0	0	0

(c) Left hemisphere, fully connected, inferior inputs

Intrinsic connections (Hz)

	iOCC	sOCC	STS	P1	P2
iOCC	-1.0000	0.0932	0.0469	0.1218	0.1214
sOCC	0.2992	-1.0000	0.0526	0.1286	0.1107
STS	0.1279	0.0507	-1.0000	0.0823	0.0887
P1	0.3224	0.1584	0.0970	-1.0000	0.1991
P2	0.2984	0.1315	0.0968	0.1898	-1.0000

Probability for intrinsic connections (p-value)

	iOCC	sOCC	STS	P1	P2
iOCC	NaN	1.0000	0.9953	1.0000	1.0000
sOCC	1.0000	NaN	0.9985	1.0000	1.0000
STS	0.9984	0.9968	NaN	0.9999	1.0000
P1	1.0000	1.0000	0.9999	NaN	1.0000
P2	1.0000	1.0000	0.9999	1.0000	NaN

Variance for intrinsic connections (Hz^2)

	iOCC	sOCC	STS	P1	P2
iOCC	0	0.0030	0.0076	0.0034	0.0058
sOCC	0.0072	0	0.0070	0.0028	0.0029
STS	0.0419	0.0079	0	0.0090	0.0096
P1	0.0106	0.0042	0.0132	0	0.0077
P2	0.0133	0.0032	0.0124	0.0056	0

Number of controls with intrinsic connections at a significance of 95% or greater

	iOCC	sOCC	STS	P1	P2
iOCC	0	1	1	1	2
sOCC	22	0	0	1	0
STS	18	0	0	2	2
P1	26	2	0	0	9
P2	22	0	3	6	0

Modulatory connections (Hz)

	iOCC	sOCC	STS	P1	P2
iOCC	0	-0.0141	-0.0103	-0.0171	-0.0204
sOCC	-0.0337	0	-0.0282	-0.0458	-0.0473
STS	0.0371	0.0159	0	0.0234	0.0307
P1	0.0523	0.0102	0.0059	0	0.0164
P2	0.1057	0.0359	0.0289	0.0555	0

Probability for modulatory connections (p-value)

	iOCC	sOCC	STS	P1	P2
iOCC	NaN	0.0240	0.1390	0.0865	0.0892
sOCC	0.0024	NaN	0.0000	0.0000	0.0000
STS	0.9884	0.9976	NaN	0.9952	0.9993
P1	1.0000	0.9956	0.9285	NaN	0.9942
P2	1.0000	1.0000	1.0000	1.0000	NaN

Variance for modulatory connections (Hz^2)

	iOCC	sOCC	STS	P1	P2
iOCC	0	0.0013	0.0023	0.0040	0.0059
sOCC	0.0032	0	0.0009	0.0010	0.0011
STS	0.0064	0.0007	0	0.0019	0.0020
P1	0.0019	0.0004	0.0004	0	0.0010
P2	0.0059	0.0011	0.0010	0.0014	0

Number of controls with modulatory connections at a significance of 95% or greater

	iOCC	sOCC	STS	P1	P2
iOCC	0	0	0	0	0
sOCC	0	0	0	0	0
STS	1	0	0	0	0
P1	0	0	0	0	0
P2	2	0	0	0	0

(d) Left hemisphere, no sOCC, not fully connected, inferior inputs (same as fully connected cascade)

Intrinsic connections (Hz)

	iOCC	STS	P1	P2
iOCC	-1.0000	0.1144	0	0
STS	0.3112	-1.0000	0.1400	0.1383
P1	0	0.3041	-1.0000	0.3093
P2	0	0.2641	0.3036	-1.0000

Probability for intrinsic connections (p-value)

	iOCC	STS	P1	P2
iOCC	NaN	0.9951	NaN	NaN
STS	0.9997	NaN	1.0000	1.0000
P1	NaN	0.9996	NaN	1.0000
P2	NaN	0.9992	1.0000	NaN

Variance for intrinsic connections (Hz^2)

	iOCC	STS	P1	P2
iOCC	0	0.0454	0	0
STS	0.1763	0	0.0196	0.0229
P1	0	0.1708	0	0.0351
P2	0	0.1498	0.0305	0

Number of controls with intrinsic connections at a significance of 95% or greater

	iOCC	STS	P1	P2
iOCC	0	5	0	0
STS	24	0	4	2
P1	0	22	0	16
P2	0	23	16	0

Modulatory connections (Hz)

	iOCC	STS	P1	P2
iOCC	0	-0.0171	0	0
STS	0.0747	0	0.0067	0.0108
P1	0	0.0224	0	0.0069
P2	0	0.0596	0.0615	0

Probability for modulatory connections (p-value)

	iOCC	STS	P1	P2
iOCC	NaN	0.1980	NaN	NaN
STS	0.9977	NaN	0.6966	0.7696
P1	NaN	0.9091	NaN	0.7090
P2	NaN	0.9956	1.0000	NaN

Variance for modulatory connections (Hz^2)

	iOCC	STS	P1	P2
iOCC	0	0.0106	0	0
STS	0.0157	0	0.0045	0.0056
P1	0	0.0072	0	0.0041
P2	0	0.0119	0.0034	0

Number of controls with modulatory connections at a significance of 95% or greater

	iOCC	STS	P1	P2
iOCC	0	1	0	0
STS	2	0	0	0
P1	0	0	0	0
P2	0	0	0	0

(e) Left hemisphere, p2-output

Intrinsic connections (Hz)

	iOCC	STS	P1	P2
iOCC	-1.0000	0.1357	0	0
STS	0.3222	-1.0000	0.2096	0
P1	0	0.4139	-1.0000	0.2678
P2	0	0	0.5126	-1.0000

Probability for intrinsic connections (p-value)

	iOCC	STS	P1	P2
iOCC	NaN	0.9981	NaN	NaN
STS	0.9997	NaN	1.0000	NaN
P1	NaN	0.9997	NaN	1.0000
P2	NaN	NaN	1.0000	NaN

Variance for intrinsic connections (Hz^2)

	iOCC	STS	P1	P2
iOCC	0	0.0491	0	0
STS	0.1849	0	0.0410	0
P1	0	0.3086	0	0.0348
P2	0	0	0.0662	0

Number of controls with intrinsic connections at a significance of 95% or greater

	iOCC	STS	P1	P2
iOCC	0	6	0	0
STS	24	0	13	0
P1	0	23	0	11
P2	0	0	23	0

Modulatory connections (Hz)

	iOCC	STS	P1	P2
iOCC	0	-0.0158	0	0
STS	0.0693	0	0.0181	0
P1	0	0.0453	0	0.0022
P2	0	0	0.1302	0

Probability for modulatory connections (p-value)

	iOCC	STS	P1	P2
iOCC	NaN	0.1995	NaN	NaN
STS	0.9969	NaN	0.8362	NaN
P1	NaN	0.9696	NaN	0.5745
P2	NaN	NaN	1.0000	NaN

Variance for modulatory connections (Hz^2)

	iOCC	STS	P1	P2
iOCC	0	0.0091	0	0
STS	0.0146	0	0.0089	0
P1	0	0.0144	0	0.0037
P2	0	0	0.0077	0

Number of controls with modulatory connections at a significance of 95% or greater

	iOCC	STS	P1	P2
iOCC	0	0	0	0
STS	2	0	1	0
P1	0	1	0	0
P2	0	0	2	0

(f) Left hemisphere, p1-output

Intrinsic connections (Hz)

	iOCC	STS	P1	P2
iOCC	-1.0000	0.1242	0	0
STS	0.3008	-1.0000	0	0.1955
P1	0	0	-1.0000	0.5335
P2	0	0.3865	0.2800	-1.0000

Probability for intrinsic connections (%)

	iOCC	STS	P1	P2
iOCC	NaN	0.9967	NaN	NaN
STS	0.9995	NaN	NaN	1.0000
P1	NaN	NaN	NaN	1.0000
P2	NaN	0.9995	1.0000	NaN

Variance for intrinsic connections (Hz^2)

	iOCC	STS	P1	P2
iOCC	0	0.0478	0	0
STS	0.1757	0	0	0.0438
P1	0	0	0	0.0891
P2	0	0.2969	0.0407	0

Number of controls with intrinsic connections at a significance of 95% or greater

	iOCC	STS	P1	P2
iOCC	0	6	0	0
STS	24	0	0	11
P1	0	0	0	22
P2	0	22	13	0

Modulatory connections (Hz)

	iOCC	STS	P1	P2
iOCC	0	-0.0165	0	0
STS	0.0728	0	0	0.0214
P1	0	0	0	0.0346
P2	0	0.0608	0.0192	0

Probability for modulatory connections (p-value)

	iOCC	STS	P1	P2
iOCC	NaN	0.1870	NaN	NaN
STS	0.9956	NaN	NaN	0.8693
P1	NaN	NaN	NaN	0.9776
P2	NaN	0.9872	0.9444	NaN

Variance for modulatory connections (Hz^2)

	iOCC	STS	P1	P2
iOCC	0	0.0090	0	0
STS	0.0178	0	0	0.0094
P1	0	0	0	0.0073
P2	0	0.0178	0.0037	0

Number of controls with modulatory connections at a significance of 95% or greater

	iOCC	STS	P1	P2
iOCC	0	1	0	0
STS	2	0	0	1
P1	0	0	0	1
P2	0	1	0	0